Numerical Simulation and Experimental Research on Rubber Flexible-Die Forming Limitation with New Position-Limited Back Pressure Mechanism

Zhi-ren Han (hanren888@163.com)
Shenyang Aerospace University https://orcid.org/0000-0001-5873-6174
Chuang Wei
Shenyang Aerospace University
Si-min Du
Shenyang Aerospace University
Zhen Jia
Shenyang Aerospace University
Xin-yang Du
Shenyang Aerospace University

Research Article

Keywords: T-shaped tube forming, Rubber flexible-die forming, Position-limited back pressure mechanism, Forming limitation, Thickness distribution

Posted Date: March 5th, 2021

DOI: https://doi.org/10.21203/rs.3.rs-269380/v1

Version of Record: A version of this preprint was published at The International Journal of Advanced Manufacturing Technology on July 6th, 2021. See the published version at https://doi.org/10.1007/s00170-021-07583-5.

Numerical Simulation and Experimental Research on Rubber Flexible-Die Forming Limitation with New Position-Limited Back Pressure Mechanism

Zhiren Han*, Chuang Wei, Simin Du, Zhen Jia, Xinyang, Du

Key Laboratory of Fundamental Science for National Defence of Aeronautical Digital Manufacturing Process, Shenyang Aerospace University, Shenyang 110136, China
*Corresponding author: TEL: +8602489723714 E-mail Address: hanren888@163.com

Abstract: The forming limitation and the wall thickness distribution are two main parameters for estimating the forming quality of T-shaped tube. In this paper, the effects of three key factors on the forming limitation and the wall thickness distribution are investigated, which are punch front distance l_1, reverse height h_1 and matching relationship between rubber hardness and axial feed Δl. A new position-limited back pressure mechanism is proposed which is made up of rigid position-limited lever, flexible back pressure medium and rigid spacer. The simulations and experiments are carried out. Both results show the thinning rate of the wall thickness decreases first and then increases and the thickening rate decreases gradually with the increase of l_1. The branch reaches the highest with the l_1 of 5mm under the requirements of thinning rate and thickening rate. With the increase of reverse height h_1, the bigger h_1 is beneficial to the wall thickness thinning suppress at the top of branch, the highest branch was formed when h_1 is 7mm. When Δl is fixed, the rubber hardness has a great influence on the forming defects, higher rubber hardness causes the top of branch to rupture and lower causes the wall to wrinkle. When rubber hardness is fixed, the thickening rate decreases with the increase of Δl. The best forming limitation and thickness distribution are achieved with the punch front distance l_1 of 5mm, the reverse height h_1 of 7mm, the rubber hardness of 70HA and the axial feed Δl of 24mm.

Key Words: T-shaped tube forming; Rubber flexible-die forming; Position-limited back pressure mechanism; Forming limitation; Thickness distribution;

1. Introduction

Internal high-pressure forming technology is one of the plastic forming processes which can transform tube blanks into T-shaped components using high-pressure liquid as bulging medium. It is widely used for manufacturing hollow structural parts in aerospace, automotive industries and many other manufacturing fields. It has many advantages compared with traditional T-shaped tube forming technologies such as welding which has great damage to the mechanical performance of tube and welded products increase the weight of tube [1]. The products formed by internal high-pressure usually have high-strength, stiffness and high-quality surfaces with lightweight [2]. Simple and low-cost rubber forming mechanism can manufacture parts with complex shapes [3].

In recent years, many researchers proposed different advanced approaches to produce tube parts based on internal high-pressure forming technology. Dond et al [4] applied the electromagnetic method and studied the effect of coil-workpiece magnetic coupling coefficient on the forming process. Lv et al [5] greatly improved the accuracy of part shapes by controlling parameters such as discharge frequency and energy. Kristoffer et al [6] and Ray et al [7] respectively carried out a complete simulation of forming process by using finite element technology, and understood the flow of metal materials more intuitively through the changes of location of element nodes. Accurate control of bulging forming force in forming process is the key factor of affecting the results. Feng et al [8] used DYNAFORM software to simulate the forming process and studied the forming

performance under different loading paths and analyzed the influence of main factors on the hydroforming formability by using response surface method. Nikhare [9] believed that bulging force is related to yield stress. Nakamori [10] built sensors into the mold cavity of control system to improve the accuracy of branch tube protrusion. In the process of deformation, the friction generated by the inner wall of the tube billet is an important factor that impedes the flow of the material. Dai [11] use different lubricants to perform memory experiments on the local forming area, which improves the forming efficiency. The studies about internal high-pressure forming technology mentioned above have been developed widely in manufacturing, but there are still some shortcomings to be improved since they require a complete seal device and the whole experiment needs special equipment and complex control system.

Nowadays, more advanced methods of using polyurethane rubber as forming medium have been developed to achieve T-shaped tube [12]. The rubber flexible-die forming technology has many advantages in manufacturing parts with complex shapes and tube will generate deformation and fit the rigid die [13]. Polyurethane rubber rod can be quickly restored to its original state and removed from the external force and it is easy to take out from the workpiece, which can be recycled and reused. Based on this, bulging the T-shaped tube with rubber medium can ignore the airtightness of the equipment and the experiment can be completed on general stamping machine. Zhang et al [14] carried out electro-hydraulic forming experiments with flexible-die, analyzed the advantages and disadvantages of flexible-die and proved the importance of improving the smoothness of die surface in forming. Girard [15] combined simulation and experimental analysis and concluded that the stress of metal during plastic deformation is irregular. Omid [16] proposed a rubber pad tube straining technology.

With the developments of rubber flexible-die forming technology, compound bulging forming has been developed. In the research of compound bulging of tube, there are two traditional methods of adding back force which are rigid mechanism and flexible mechanism. Chen [17] added a back pressure punch to the top of the branch tube. After it formed to a certain height, the punch began to apply a balanced back pressure, which increased the deformation of the material. Zou [18] found that the height of the branch increased first and then decreased with the increase of back pressure time. Therefore, the back pressure is the key factor which can influence the height of T-tube branch and distribution of wall thickness in compound bulging forming. In the studies above, the back pressure has been proved to play an important role in compound bulging forming, but the back pressure device is not described in studies. In traditional compound bulging forming, a hydraulic pressure system will be set as the back pressure mechanism at the branch to provide back pressure, and the punches move along the direction of branch through control system, but it is not convenient because of adding experimental cost and processing steps, and also it is hard to control the time of adding back pressure which can influence the height of branch. Besides, there will be failures such as wrinkle and rupture and the T-shaped tube cannot be processed further so that the T-shaped tube formed by traditional bulging mechanism cannot be applicated in aerospace completely. Therefore, it is necessary to design a new back pressure mechanism for rubber compound bulging forming.

In this study, the rubber flexible-die compound bulging forming method was developed with a new position-limited back pressure mechanism designed for T-shaped tube forming by numerical simulation and experiments. The influence of three key factors on forming limitation (forming height of T-shaped tube branch) and the wall thickness distribution are investigated, and the main three factors are included with the punch front distance l_1, the reverse height h_1 and the matching relationship between rubber hardness and axial feed Δl. The finite element model of T-shaped tube was established and the compound bulging forming simulations and experiments were carried out.

Through results obtained from simulations and experiments, the accuracy of FEM was verified compared with experiments and the influence of influencing factors on forming limitation and wall thickness distribution was studied and the best forming scheme can be achieved in this study.

2 Methodology

2.1 Compound Bulging Forming Principle

The cavity of the T-shaped tube bulging can be divided into three zones according to mechanical characteristics as shown in Fig.1: (A) Guiding zone, (B) Transition zone and (C) Expansion zone.

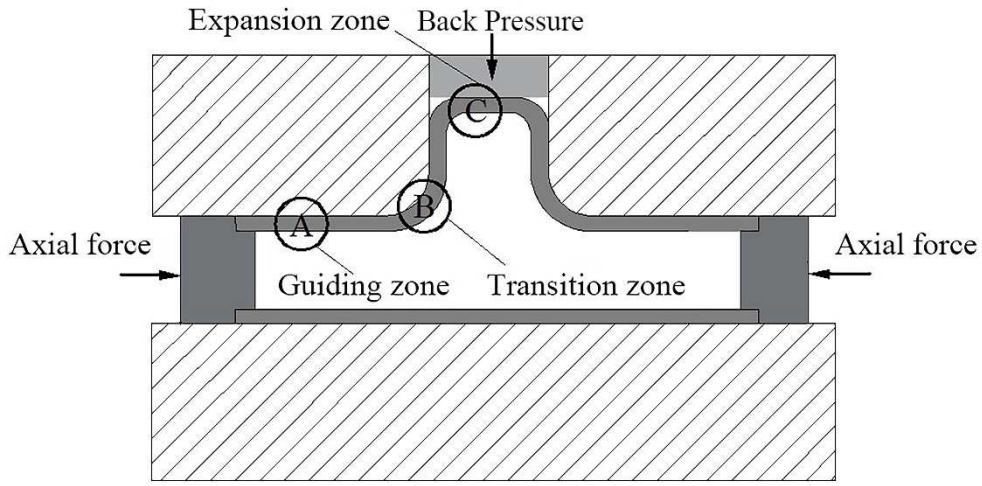

Fig.1. Principle of T-shaped Tube Compound Bulge Forming

The rubber rod expands under the action of axial feed to generate internal pressure, and the tube enters the stage of plastic deformation in zone A (Guiding zone). As internal pressure increases, the metal material flows along mold cavity to form the branch of tube in zone B (Transition zone). In order to prevent rupturing in zone C (Expansion zone), back pressure rubber is set in the position-limited back pressure mechanism to apply a back pressure to suppress the wall rupturing at the top of branch. The compound bulging forming mechanical state is shown in Fig.2 [19].

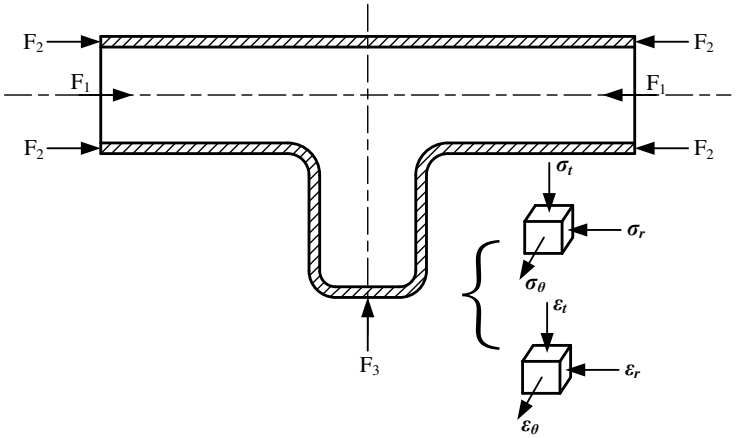

Fig.2. Compound Bulging Mechanical State

As shown in Fig.2, the compounding bulging mechanical state includes three parts: F_1 acts on the end faces of rubber rod, F_2 acts on the end faces of tube and F_3 represents the reverse force acting

in expansion zone. Under the effect of “internal force-axial force-longitudinal force”, the height of T-shaped tube branch and the wall thickness distribution can be improved.

2.2 Forming Processing

The mechanism of tube compound bulging forming mechanism with polyurethane rubber are shown in Fig.3 (1-die, 2-axial punches, 3-tube, 4-polyurethane rubber rod, 5-rigid position-limited lever, 6-rigid spacer, 7-flexible back pressure medium).

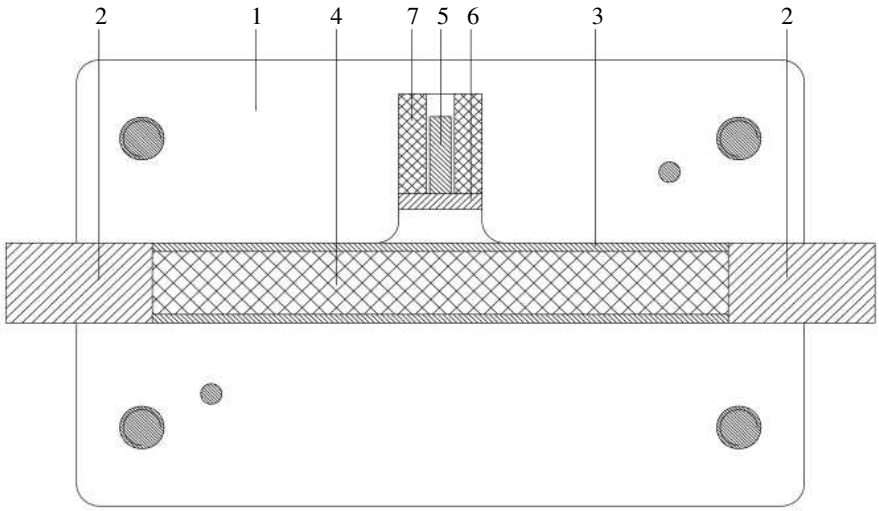

Fig.3. Compound Bulging Forming Mechanism of Original State

The forming process can be described as follows:

(1) Before experiments, the faces of tube and die cavity are buffed by abrasive paper and smeared with lube to decrease friction. The dies are put on workbench and the tube, polyurethane rubber rod and position-limited back pressure mechanism are assemble as shown in Fig.3, and then start the hydraulic press machine.

(2) During forming, the front faces of punches contact the polyurethane rubber rod first and then with the feed of axial punches, the behind faces of punches contact tube and the tube is compressed along the axial direction. With the action of F_1 and F_2 together, the materials of tube flow to the free space of the die cavity gradually to form the branch.

(3) With the increase of deformation, the top of branch contact to the position-limited back pressure mechanism and the back pressure mechanism provides back pressure F_3 to balance internal force F_1 and axial force F2 to suppress thinning and avoid rupturing. The tube generates plastic deformation under the action of F_1, F_2 and F_3 together.

(4) Stop feeding when the height of branch reaches the ideal height, draw back the punches and open dies to take out the T-tube to finish bulging forming.

The model of T-shaped tube after forming is shown in Fig.4.

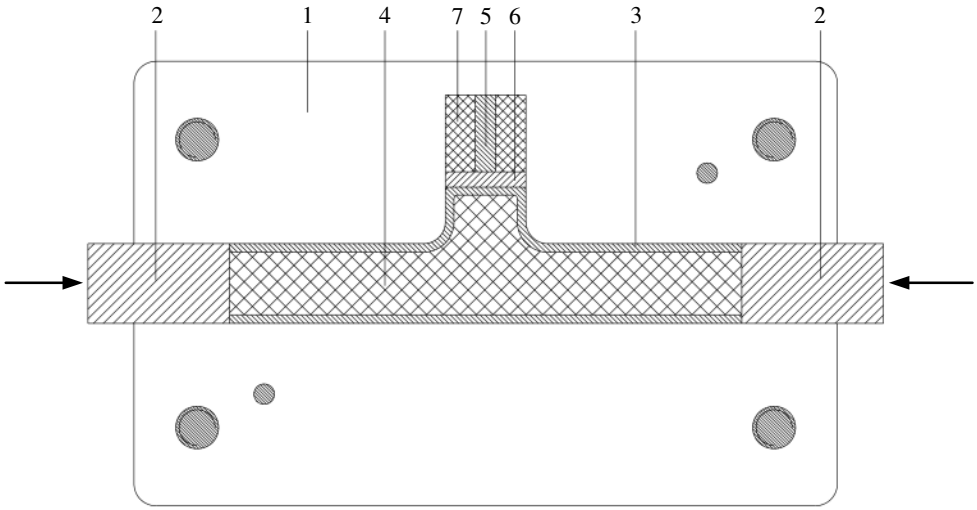

Fig.4. Compound Bulging Forming State After Forming

2.3 Main Influence Factors

2.3.1 Punch Front Distance l_1

During forming, the function of both axial punches is to provide axial compressive force, the structural parameters of punches in study are shown in Fig.**5**.

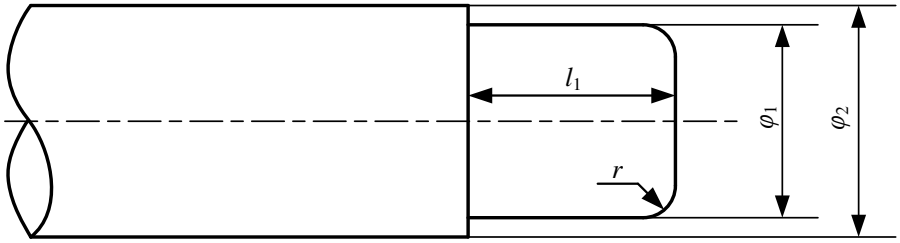

Fig.5. Schematic diagram of punch structure

The punch front diameter φ_1 is same as the diameter of rubber rod, punch outer diameter is same as the outer diameter of tube blank. The punch front surface is chamfered with r=0.25mm to prevent the rubber surface from being damaged by punch extrusion. The front face of punch contacts the face of rubber rod first and then during forming, the punches add force to rubber rod and tube in proper order. The larger l_1 is the later the bulging zone will be refilled, and the pressure acting on the inner cavity of tube will increase too fast and the wall thickness will reduce rapidly. The smaller l_1 is the earlier the bulging zone will be refilled, in the initial period of experiment, the internal pressure is too small to support the deformation of tube and on the contrast the filling will suppress the forming. Therefore, the punch front distance l_1 is an important factor and the impact of the punch front distance l_1 on forming results will be analyzed.

2.3.2 Reverse Height h_1

During compound bulging forming, the back pressure is an important factor to influence the forming limitation and suppress rupturing on the top of branch. A new position-limited back pressure mechanism including rigid position-limited lever, flexible back pressure medium (polyurethane rubber rod) and rigid spacer was designed as shown in Fig.6.

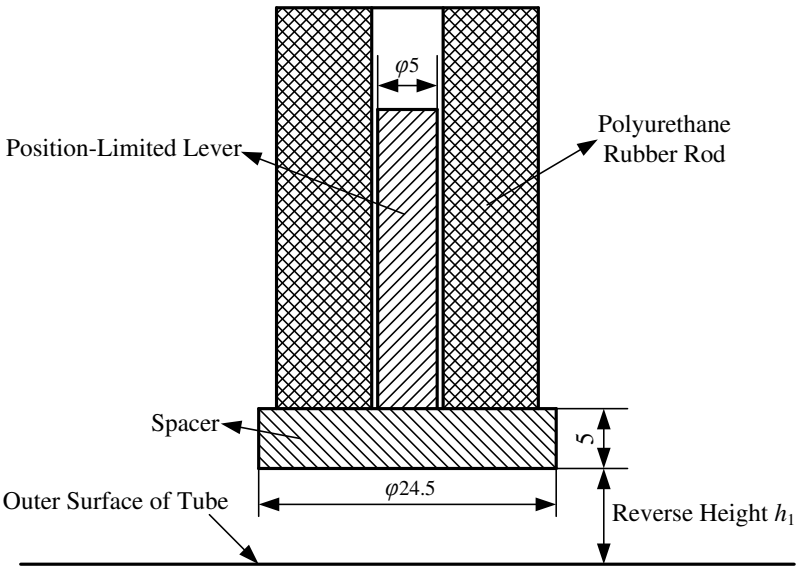

Fig.6. Schematic diagram of the position-limited back pressure mechanism

The rigid position-limited lever is fixed on the center of the rigid spacer along the bottom of branch cavity, the flexible reverse medium is designed as hollow cylindrical polyurethane rubber rod set on rigid position-limited lever. The length of flexible back pressure rubber rod is bigger than the length of rigid position-limited lever and the inner diameter of flexible back pressure rubber rod is also bigger than the diameter of rigid position-limited lever. One side of flexible back pressure rubber rod is fixed with rigid spacer and the other side is fixed at the bottom of branch cavity.

During forming, the tube is acted by the internal force and axial force together for a period time before it starts to contact longitudinal back pressure mechanism, the reverse height determines the distance between the top of branch and position-limited back pressure mechanism thereby it also determines the time when the back pressure is added to the branch. The position-limited back pressure mechanism designed in rubber forming process provide back pressure to prevent excessive deformation on the branch top, and the reverse height is one of the key factors for the T-tube bulging process to maintain a reasonable numerical relation between the internal pressure and the equilibrium force generated by the axial feed.

Compared with traditional back pressure device made up of hydraulic pressure system, the back pressure of position-limited back pressure mechanism is generated by flexible medium (polyurethane rubber rod) first, the back pressure increases gradually with compression of flexible medium and then when rigid spacer contacts rigid position-limited lever, the back pressure fixes and maintains unchanged. The working principle of the back pressure mechanism showed in Fig.6 is expressed as that the position-limited lever and the polyurethane rubber rod remains fixed firstly and then the polyurethane rubber rod will move upward under the action of spacer with the branch top contacting the bottom surface of spacer until the branch of T-shaped tube reaches the ideal height. In study, the impact of the reverse height h_1 on forming results will be analyzed.

2.3.3 Matching Relationship Between Rubber Hardness and Axial Feed (MRRHAF)

The matching relationship between rubber hardness and feed of axial punches is named as load path, the rubber hardness and the feed of axial punches are the key factors. Therefore, it is necessary to explore a reasonable load path.

During forming, the internal force is generated by compress of polyurethane rubber rod under the action of axial punches, the internal force generated from rubber rod is related to the hardness

of rubber rod and its properties. Polyurethane rubber is a typical nonlinear material with excellent material properties such as high elasticity, good flexibility, high liquidity and so on. Rubber hardness is a measure of the adhesive viscosity characteristics, processable properties and compression characteristics and other aspects of the performance of the comprehensive material index. As a medium of transferring force, the rubber hardness directly affects the pressure of the inner wall of the tube, as well known the axial feed also has a great influence on the pressure in the tube. Therefore, the matching relationship between the rubber hardness and axial feed (MRRHAF) is another important factor to the study on the T-tube bulging forming.

The polyurethane rubber hardness and force energy relationship can be described by Mooney-Rivlin model as listed in equation (1) [20, 21]. The material theoretical coefficients C_{10} and C_{01} obtained by fitting elongation and stress-strain data, the main energy density function can be expressed as:

$$W_R = \sum_{i,j=0}^{\infty} C_{ij} \left(I_1 - 3\right)^i \left(I_2 - 3\right)^j \tag{1}$$

Where I_1 and I_2 represent strain invariants, equation (1) can be simplified as:

$$W = C_{10}\left(I_1 - 3\right) + C_{01}\left(I_2 - 3\right) \tag{2}$$

The relationship between principal stress σ and principal elongation ratio λ can be obtained as follows:

$$\sigma = 2\left(\lambda - \frac{1}{\lambda^2}\right)\left(\frac{\partial W}{\partial I_1} + \frac{1}{\lambda}\frac{\partial W}{\partial I_2}\right) \tag{3}$$

Where λ=1+ε

Equation (4) will be obtained with combining elongation λ and stress value σ:

$$C_{10} + \frac{1}{\lambda}C_{01} = \frac{\sigma}{2\left(\lambda^2 - \frac{1}{\lambda}\right)} \tag{4}$$

In study of load path, the feed of axial punches is another important influence factor. Based on the assumption that the wall thickness before and after deformation is completed unchanged, the ideal feed can be estimated as follows [22, 23]:

$$\Delta l = L_0 - L_1 = \frac{Dl}{d} + \frac{D^2 - d^2}{2d\sin\alpha} - L \tag{5}$$

Where L_0 is the original length of tube, L_1 is the length of tuber after forming, L is the length of tube in forming zone (expansion zone), the length of maximum diameter is l=L-(D-d)/tanα, α represents transition fillet, d is inner diameter and D is outer diameter of tube.

The impact of matching relationship between rubber hardness and axial feed (MRRHAF) will be analyzed.

3 Numerical Simulation on Rubber Flexible-Die Forming of Tube

3.1 Finite Element Model

In study, the process of tube rubber flexible-die forming was numerical simulated by using finite element software ANSYS Workbench, the geometry models were built by CATIA and imported into ANSYS Workbench. The model was simplified with dies, tube, forming medium (polyurethane rubber rod), axial punches and position-limited back pressure mechanism according to the bulging methodology. During simulation, the dies, axial punches and rigid position-limited lever and rigid spacer were regarded as rigid body without deformation, the tube, polyurethane rubber rod and flexible reverse medium were regarded as flexible body.

The material of tube is Brass H85 and the material properties are shown in Table 1.

Table 1. Material Properties of Brass H85

Mechanical Properties	Value
Density / kg·m^{-3}	8750
Young's Modules / MPa	119000
Poisson's Ratio	0.3
Yield Strength / MPa	305
Tangent Modulus / MPa	590

The original length L_0 of tube in finite element simulation can be calculated as follows [24]:

$$L_0 = L_t + h - \frac{4\left(D^2 + Dd + d^2\right)}{3\pi\left(D + d\right)} + \frac{d^2}{2\left(D + d\right)} \tag{6}$$

Where L_t is the length of tube at a certain time during forming, h is the height of branch, d is inner diameter and D is the outer diameter of tube. Through initial simulation, the length of tube in finite element simulation is 120mm, the outer diameter of tube is 24mm and the inner diameter of tube is 21mm.

Three hardness (60HA,75HA and 90HA) of polyurethane rubber rods are selected as bulging medium in simulation, the length of rubber rod l_0 is 118mm and the diameter d_0 is 20mm. The theoretical Mooney-Rivlin coefficients are shown in Table 2.

Table 2. Theoretical Coefficients of Polyurethane Rubber

Rubber Hardness	C_{10} / MPa	C_{01} / MPa
60HA	0.302	0.076
75HA	0.736	0.184
90HA	2.824	0.706

In ANSYS Workbench LS-DYNA module, the geometry models were assigned with corresponding materials and meshed. In simulation, in order to improve calculation speed, the rigid bodies such as dies, axial punches, rigid position-limited lever and rigid spacer can be meshed rough appropriately, while the flexible bodies such as tube, polyurethane rubber rod and flexible back pressure medium were meshed fine. The dies were fixed with the limitation of six degrees, the position-limited back pressure mechanism moved only along the parallel direction of branch and

the axial punches moved only along the horizontal direction of cavity. The contacts during forming were satisfied with Coulomb's laws of sliding friction, the friction coefficient between the outer face of tube and the inner face of die cavity was set as 0.1 and the friction coefficient between the rubber and the inner face of tube was set as 0.25. According to equation (5), the ideal axial feed Δl was calculated as 31.4mm. In fact, however, the factual feed is a little smaller than the ideal feed and 70%-80% of ideal feed, the factual feed was about 21.98mm-25.12mm, the feed Δl can be chosen from 23mm, 24mm and 25mm respectively. The loading velocity of axial punches can be shorted appropriately and the simulation time was set 0.1s to save simulation total time.

3.2 Analysis on Finite Element Simulation Results

The T-tube forming results were analyzed based on the height of T-tube branch and the wall thickness distribution along the longitudinal cross section and horizontal cross section of T-tube. During forming experiments, both the allowable wall thickness thickening rate and thinning rate are no more than 30% which is considered as the qualified area. Excessive thickness is not conductive to the flow of liquid and increases the weight of parts. The maximum thinning rate and the maximum thickening rate can be defined as follows [25, 26]:

$$\begin{cases} \delta_1 = \dfrac{t - t_{\min}}{t} \times 100\% = \left(1 - \dfrac{t_{\min}}{t}\right) \times 100\% \\ \delta_2 = \dfrac{t_{\max} - t}{t} \times 100\% = \left(\dfrac{t_{\max}}{t} - 1\right) \times 100\% \end{cases} \tag{7}$$

Where t represents the wall thickness, $t_{\min}$ is the minimum wall thickness and $t_{\max}$ is the maximum wall thickness.

In simulation, the deformation cloud figures along the branch direction (axis-Z) shows the distribution of displacements along branch (axis-Z), the maximum value of displacement represents the height of T-shaped tube branch. The T-shaped tube formed in simulation can be sliced along longitudinal cross section and horizontal cross section, and forty points can be defined and obtained along the outer wall from top to bottom of tube. The wall thickness of T-shaped tube along long longitudinal cross section and horizontal cross section can be measured as shown in Fig.7.

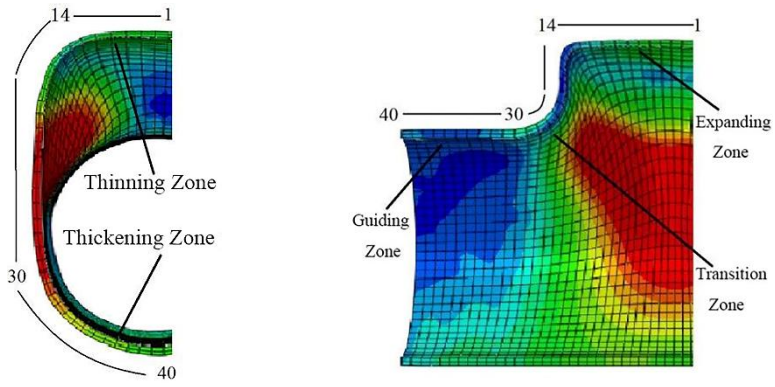

(b) Longitudinal Cross Section **(c) Horizontal Cross Section**

Fig.7. Cross Section of T-tube in Simulation

3.2.1 Effect of Punch Front Distance l_1

In simulation, three different parameters of punch front distance l_1 were set as 3.5mm, 5mm and 6.5mm respectively, the polyurethane rubber rod hardness was selected with 60HA, the feed of

axial punches was set Δl=23mm, the reverse height h_1 was 7mm and other corresponding process parameters remain unchanged.

The z-displacement cloud figures of T-shaped tube are shown in Fig.8.

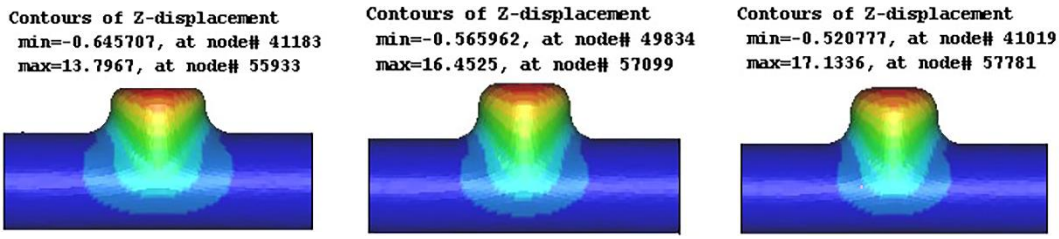

(a) l_1=3.5mm **(b) l_1=5mm** **(c) l_1=6.5mm**

Fig.8. Z-Displacement of T-shaped Tube Formed by Different Punch Front Distance l_1 in Simulation

From Fig.8, it can be found that the forming results with l_1 is 5mm and 6mm are better than it formed with l_1 is 6.5mm, and also with the increase of punch front distance l_1, the height of T-tube branch increases and when l_1 is 6.5mm the height of branch reaches the largest. The height of branch formed by different punch front distance l_1 are shown in Fig.9.

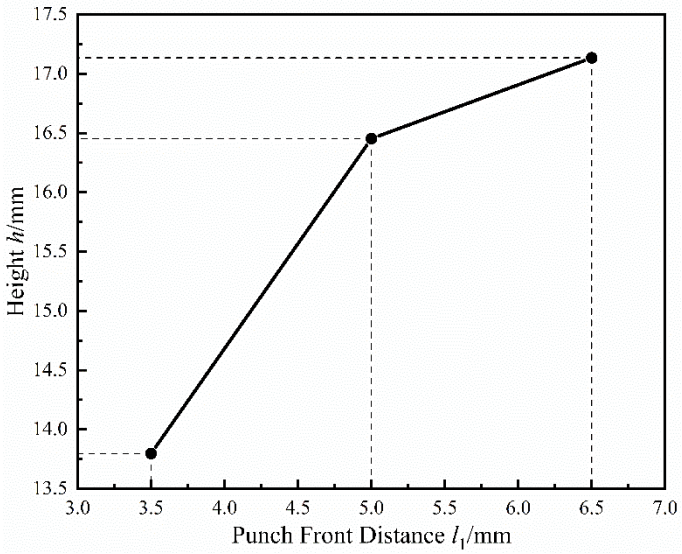

Fig.9. Height of T-shaped Tube Branch Formed by Different Punch Front Distances l_1 in Simulation

It can be found from Fig.9 that the change of T-shaped tube branch height h with the increase of punch front distance l_1, when l_1 is 3.5mm, 5mm and 6.5mm the branch height h reaches 13.797mm, 16.453mm and 17.134mm respectively. It can be drawn that the larger punch front distance can make the rubber rod compressed more adequately under the action of axial punches so that the rubber rod can generate sufficient internal pressure which is better for the height of branch, the height of branch increases with the increase of punch front distance.

The wall thickness measurement data along cross section can be measured by using the function of probe to obtain the displacement of every point and then the wall thickness can be calculated as shown in Fig.10.

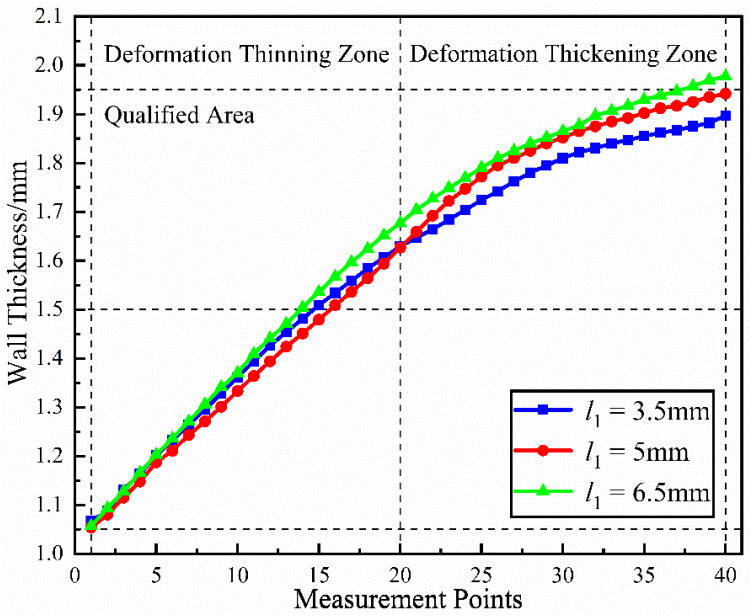

(a) Longitudinal Cross Section

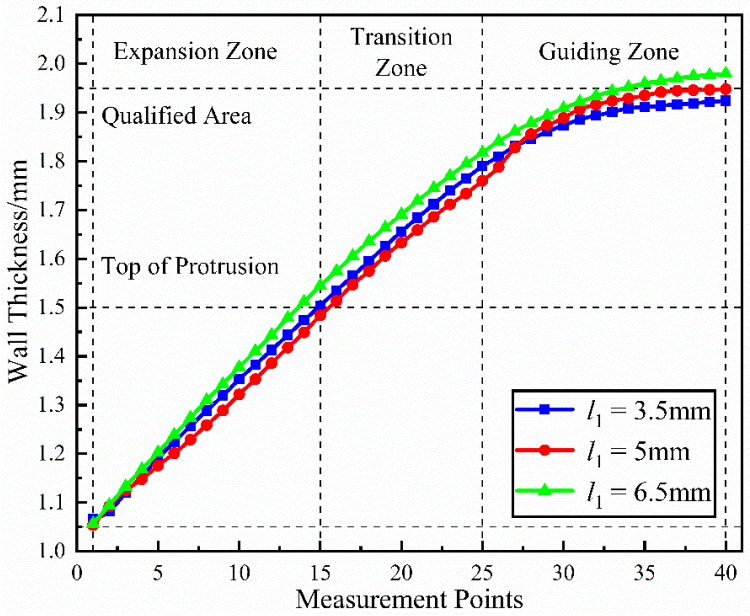

(b) Horizontal Cross Section

Fig.10. Wall Thickness Distribution of Cross Section of T-tube Formed by Different Punch Front Distance l_1 in Simulation

It can be seen from Fig.10 that in the longitudinal cross section, the wall thickness gradually increases from the top to the bottom of branch. In the horizontal cross section, the wall thickness increases in expansion and transition zone and hardly changes in the guiding zone. According to the requirements of maximum thinning rate and thickening rate, the wall thickness thickening is more than 30% in longitudinal and horizontal cross section when l_1 is 6.5mm, the wall thickness of tube is equal to requirements when l_1 is 3.5mm and 5mm, which illustrates that although larger punch front distance makes branch higher, too large punch front distance can cause the supplements of materials untimely during compression of tube and there is a risk of thinning and thickening. Combing the height of branch shown in Fig.9, the quality of T-shaped tube branch formed is higher when l_1 is 5mm. Therefore, the punch front distance l_1 as 5mm is the best in simulation.

3.2.2 Effect of Reverse Height h_1

The polyurethane rubber rod hardness is 60HA, the feed of axial punch is 23mm, the punch front distance l_1 is 5mm and other corresponding process parameters remain unchanged, and the different values of reverse height h_1 were set 3mm, 5mm, 7mm and 9mm respectively. To obtain the value of height h, the z-displacement cloud figures of T-tube are shown in Fig.11.

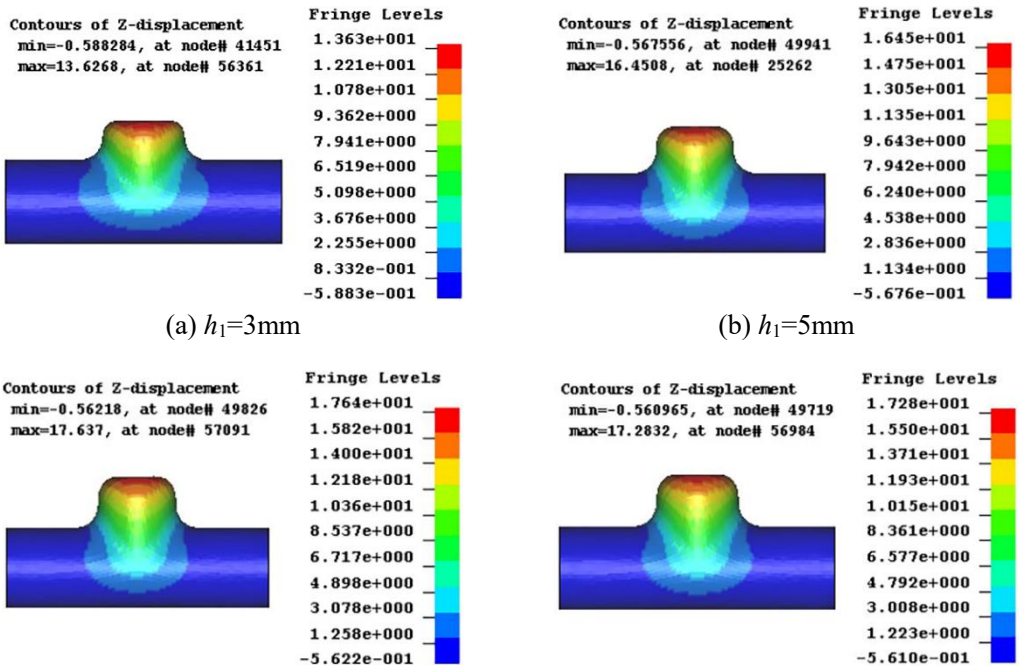

Fig.11. Z-Displacement of T-shaped Tube Formed by Different Reverse Height h_1 in Simulation

According to Fig.11, the forming height of T-tube can be obtained and shown in Fig.12.

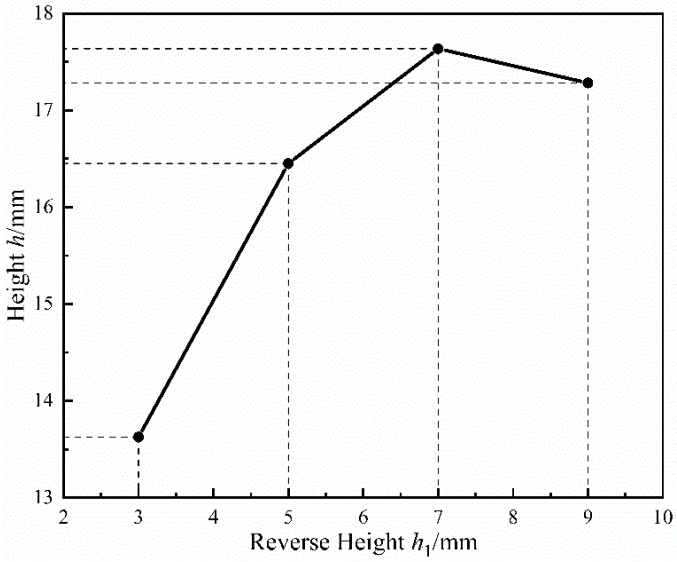

Fig.12. Height of T-shaped Tube Branch Formed by Different Reverse Height h_1 in Simulation

According to Fig.12, it can be found when h_1 is 3mm the height of branch h is 13.6268mm, when h_1 is 5mm the h is 16.4508mm, when h_1 is 7mm the h is 17.637mm and when h_1 is 9mm the h

is 17.2832mm. The following conclusion can be drawn that with the increase of reverse height h_1 the height of tube branch increases first and then decreases, when h_1 is 3mm the h is the smallest as 13.6268mm and when h_1 is 7mm the h is largest as 17.637mm. Too small reverse height will make the time short when back pressure mechanism contacts top of branch which also means adding reverse force to branch too early can cause the forming inadequately, so the height of branch cannot reach the ideal height. But with the increase of reverse height h_1, the height of branch will not increase always because of plastic performance of materials, the branch reaches the maximum height without contacting the back pressure mechanism which is same as axial compression forming. Therefore, the reverse height is not the larger the better and it has the best value, the wall thickness distribution of cross section was measured further to determine the best value as shown in Fig.13.

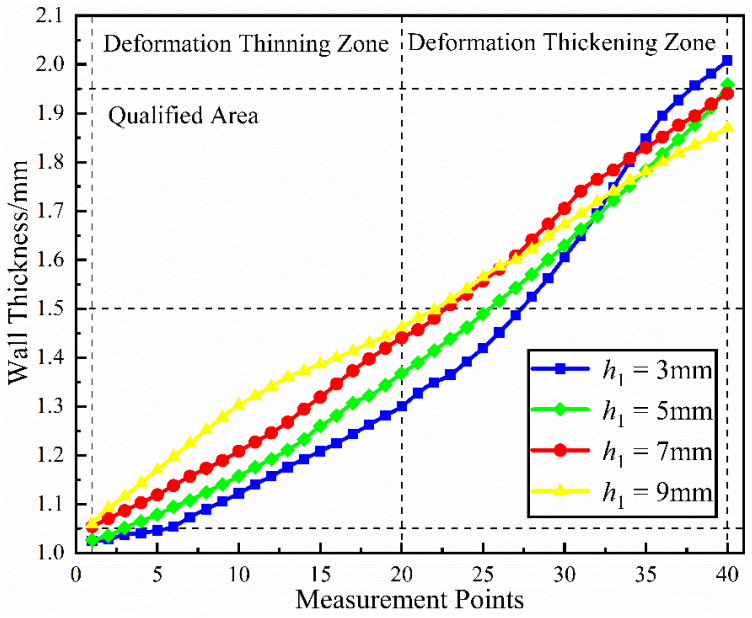

(a) Longitudinal Cross Section

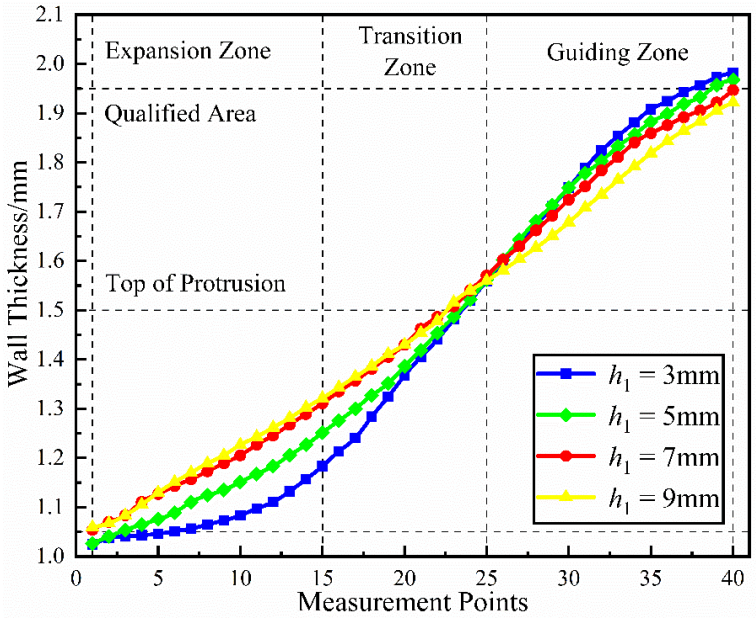

(b) Horizontal Cross Section

Fig.13. Wall Thickness Distribution of Cross Section of T-tube Formed by Different Reverse Height h_1 in Simulation

It can be found from Fig.13 that when reverse height h_1 is 3mm, the range of wall thickness is the widest, the wall thinning in the expansion zone and the wall thickening in the guiding zone seriously, and the thinning rate and thickening rate are more than 30% out of the quailed area. When reverse height h_1 is 5mm, the maximum wall thickness along horizontal cross section is 1.9589mm which is not equal to the requirements of thickening rate. When reverse height h_1 is 7mm and 9mm, the wall thickness distributes in the qualified area. With the increase of reverse height, the minimum wall thickness increases and the maximum wall thickness decreases gradually, and the smaller difference of wall thickness the thickness is more uniform. In the longitudinal and horizontal cross section, the wall thickness increases gradually, the wall thickness at top of branch decreases and increases at the bottom and both ends of tube which means the position-limited back pressure mechanism can provide reasonable back pressure to suppress the rupture and the thinning of wall thickness to help form T-tube with higher quality.

3.2.3 Effect of Load Path (MRRHAF)

Three different hardness (60HA, 75HA and 90HA) of polyurethane rubber rod were adopted and the feed of axial punches Δl were set 23mm, 24mm and 25mm respectively, and the other corresponding process parameters maintain unchanged and different load path (MRRHAF) were tested. The T-tube formed with different load paths (MRRHAF) and the z-displacement cloud figures of T-tube in simulation as shown in Fig.14.

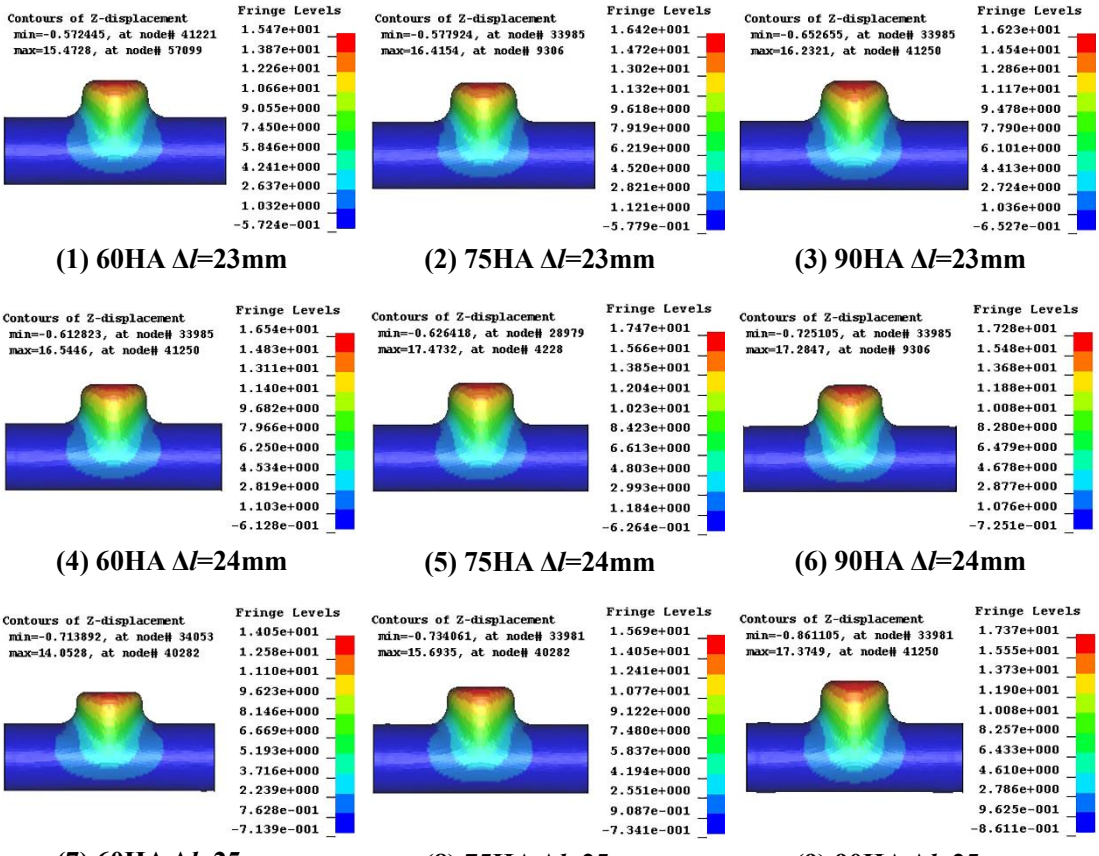

Fig.14. Z-Displacement of T-shaped Tube Formed by Different Load Path (MRRHAF) in Simulation

The forming height, maximum wall thickness and minimum wall thickness of T-shaped tube were measured and listed in Table 3.

Table 3. Results in Simulation with Different Load Paths (MRRHAF)

Number	Rubber hardness	Feed Δl/mm	Height h/mm	Thickness (Max)/mm	Thickness (Min)/mm
(1)	60HA	23	15.4728	1.9328	1.0595
(2)	75HA	23	16.4154	1.9421	1.0486
(3)	90HA	23	16.2321	1.9436	1.0364
(4)	60HA	24	16.5446	1.9469	1.0521
(5)	75HA	24	17.4732	1.8613	1.0562
(6)	90HA	24	17.2847	1.9703	1.0366
(7)	60HA	25	14.0528	1.9987	1.1025
(8)	75HA	25	15.6935	1.9792	1.0148
(9)	90HA	25	17.3749	1.9654	1.0253

Based on the requirements that the wall thickness thinning rate and thickening rate are not more than 30% which means the maximum thickness is not more than 1.95mm and the minimum thickness is not more than 1.05mm, it can be seen that the result number (1), (4) and (5) are equal to the requirements. In order to assure the quality of T-tube parts, when the wall thickness distributes uniformly the higher is branch the better to process further, so when the rubber hardness is 75HA and the feed of axial punches Δl is 24mm, the branch of T-tube reaches the highest. The wall thickness distribution measurement data of (1), (4) and (5) were shown in Fig.15.

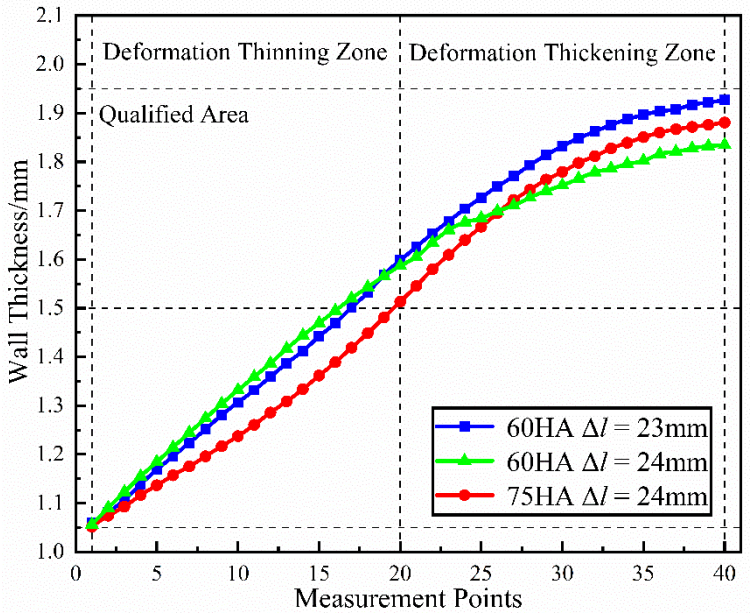

(a) Longitudinal Cross Section

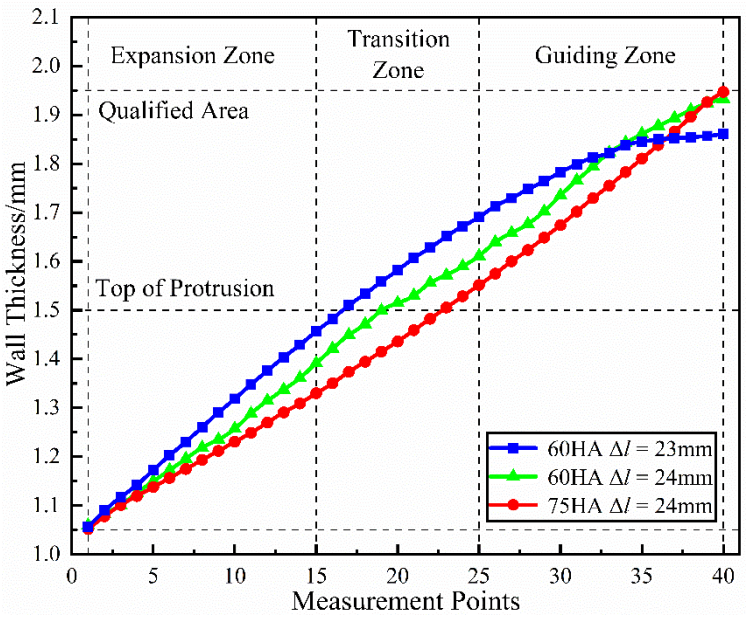

(b) Horizontal Cross Section

Fig.15. Wall Thickness Distribution of Cross Section of T-tube Formed by Different Load Paths (MRRHAF) in Simulation

It can be found from Fig.15 that from the top to the bottom of tube in horizontal cross section, the wall thickness increases, especially from expansion zone to transition zone the wall thickness increases fast and in guiding zone the increasing rate is a little slow. In the longitudinal cross section, the wall thickness decreases obviously at the top of branch. In summary, when rubber hardness is 75HA and the feed is 24mm, the thickness changes the most uniformly, therefore, combing with the height of branch, the best matching relationship between rubber hardness and feed is that rubber hardness is 75HA and feed of axial punches Δl is 24mm in this simulation.

4 Experimental Research on Rubber Compound Bulging Forming of Tube

4.1 Research Equipment and Scheme

All experiments are carried out on YQ32-400 hydraulic press. The whole experiment system consists of the hydraulic system, workbench and forming device as shown in Fig.16. The forming device consists of dies, axial punches, polyurethane rubber rod, tube and position-limited back pressure mechanism. During forming experiment, the feed speed of punch is maintained at 10mm/s. The dies are locked with the tube and polyurethane rubber rod, two axial punches synchronously applied bloating force to the rubber rod and the tube, the metal gradually entered the plastic deformation stage and began to expand along the free space of the die cavity.

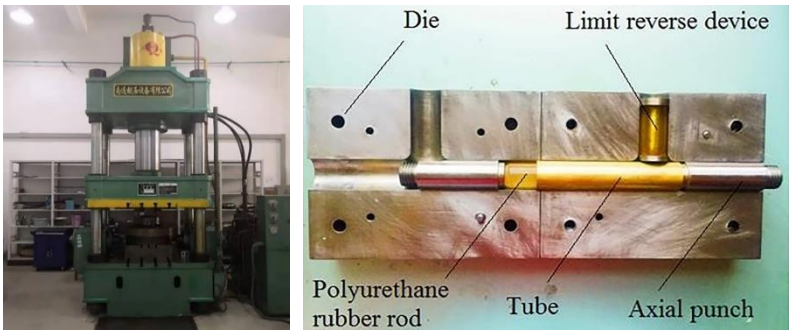

Fig.16. YQ32-400 Hydraulic Press and Forming Device

The polyurethane rubber rod (length l_0=118mm, diameter d_0=20mm) was loaded into a seamless brass H85 tube (outer diameter D=24mm, inner diameter d=21mm, tube length L_0=120mm, the wall thickness t=1.5mm). The die radius of transition zone is 7mm and the branch diameter is 24.5mm. In order to decrease the friction between outer wall of tube and inner wall of die and improve the forming performance of tube, the lubricant oil needs to be smeared on the outer wall of tube uniformly. The aerospace oil was selected as lubricant oil in this experiment because of its good compatibility of materials and it is beneficial to rubber and metal without corrosivity.

After forming, the height of T-tube branch can be measured as shown in Fig.17.

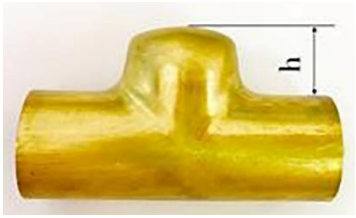

Fig.17. The Height h of T-tube Branch

The T-shaped tube was sliced by electric spark forming machine along longitudinal direction and horizontal direction as shown in Fig.18. Taking the top of the branch tube as initial position, the wall thickness gradually increases along the branch wall, and the thickening becomes more obvious as it gets closer to the end of the tube. The top of the branch tube is the area with maximum deformation in the bulging process, so it has the smallest wall thickness.

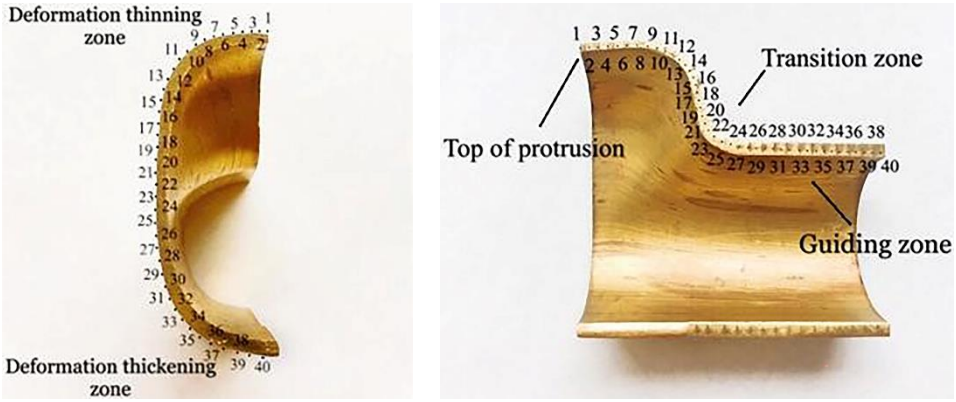

Fig.18. Cross section of T-shape tube: (a) Longitudinal cross section (b) Horizontal cross section

4.2 Analysis on Experimental Results

4.2.1 Effect of Punch Front Distance l_1

The same method and parameters in simulation were applied into experiments, the topography of the T-shaped tube formed with the three different l_1 are shown in Fig.19.

(a) l_1=3.5mm (b) l_1=5mm (c) l_1=6.5mm

Fig.19. Photography of the T-shaped Tube Formed by Different Punch Front Distances l_1

The height of T-shaped tube branch was measured according Fig.17 and the measurement data were shown in Figure 20, when l_1 is 3.5mm the height of branch h is 13.6mm, when l_1 is 5mm the height h is 15.4mm and when l_1 is 6.5mm the height h is 16.1mm. With the increase of l_1, the height of T-shaped tube branch increases, and the largest height of the branch reached 16.1mm when l_1 is 6.5mm. The larger with l_1, the better fluidity of the material which is conductive to feeding the bulging area and the height of the T-tube branch is.

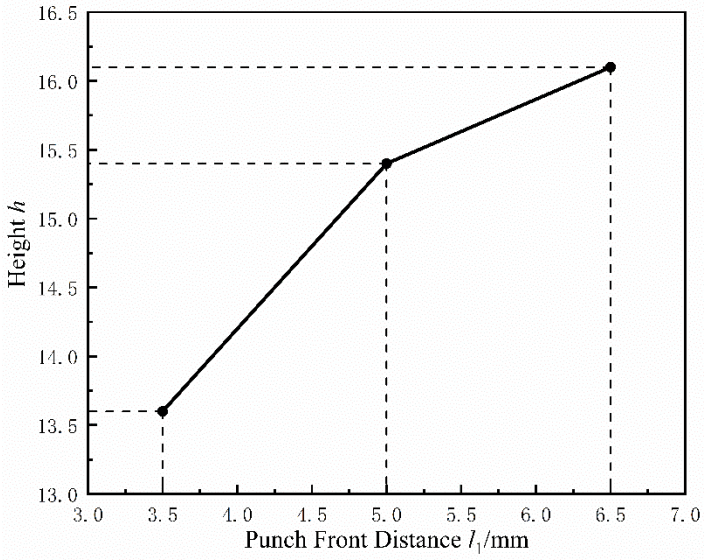

Figure 20. Height of T-shaped Tube Branch Formed by Different Punch Front Distances l_1 in Experiments

The test positions of the wall thickness on T-tube were selected as shown in Fig.18. The Wall thickness distribution on the longitudinal and horizontal cross section are expressed in Fig.21.

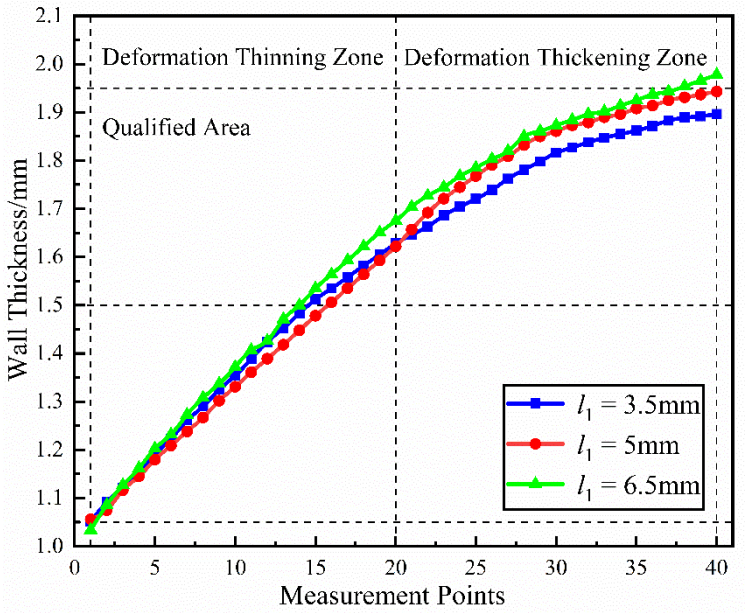

(a) Longitudinal Cross Section

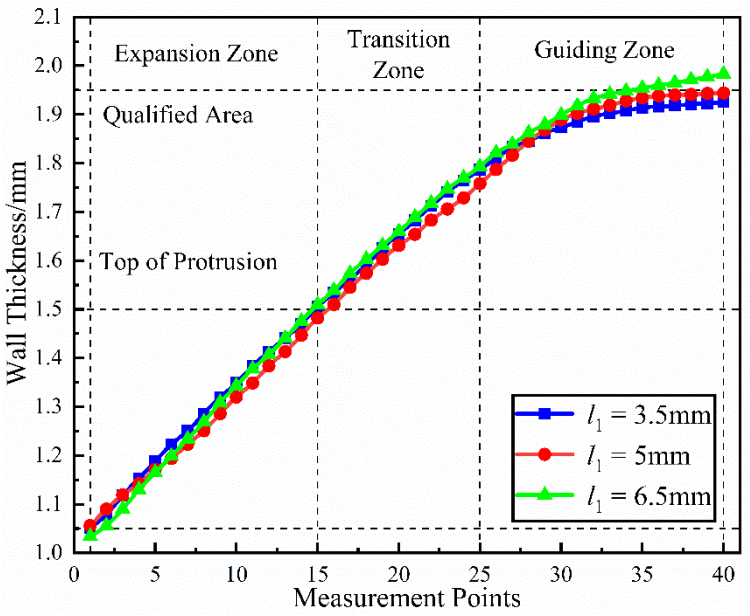

(b) Horizontal Cross Section

Fig.21. Wall Thickness Distribution of Cross Section of T-shaped Tube Formed by Different Punch Front Distances l_1 in Experiments

According to Fig.21, the wall thickness difference is the smallest when l_1 is 3.5mm and the thickness distribution is the most uniform. It can be found that when l_1 is 5mm, the maximum thickening rate decreases to about 9.6% on the longitudinal cross section, and the thinning rate significantly decreases to about 1.2% on the horizontal cross section. When l_1 is 6.5mm, the minimum wall thickness at the top can be obtained from the longitudinal profile as 1.034mm, although the largest height of the branch tube reached 16.1mm, there was a risk of rupture due to the top thinning on the branch tube and this seriously exceeded the qualified area. It can be concluded from the experiment with different punch front distances that when l_1 is 5mm the height of T-tube branch can reach the largest in the reasonable range of wall thickness thickening rate and thinning rate, so the punch front distance l_1 of 5mm is the best in experiments.

4.2.2 Effect of Reverse Height h_1

The impact of reverse height was studied with other corresponding parameters unchanged. The topography of the T-shaped tube formed with different branch heights h_1 were shown in Fig.22.

(a) h_1=3mm

(b) h_1=5mm

(c) h_1=7mm

(d) h_1=9mm

Fig.22. Photograph of T-shaped Tube Formed by Different Reverse Heights h_1 in Experiments

The height of branch can be measured and the measurement data were listed in Fig.23.

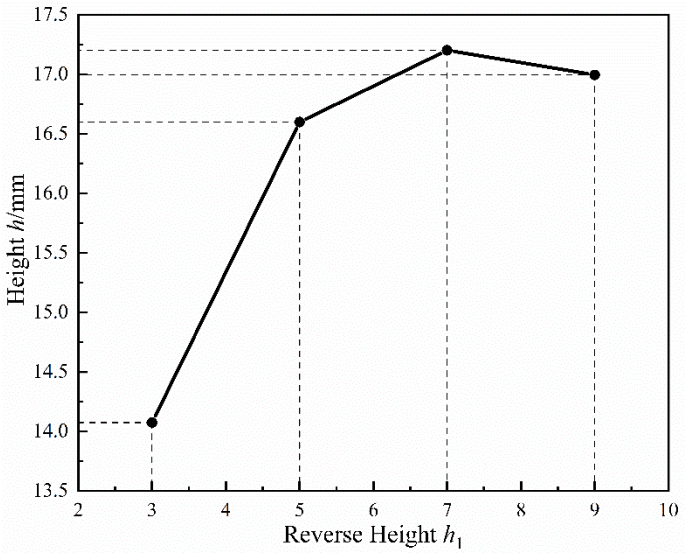

Fig.23. Height of T-shaped Tube Branch Formed by Different Reverse Height h_1 in Experiments

From Fig.23, it can be seen that the height h increases with reverse height h_1, and when h_1 is 7mm the maximum height h is formed. The reverse height h_1 determines the time when the top of the branch tube contacts the position-limited back pressure mechanism. The smaller h_1 will result in a longer time of unilateral bulging force on the top of the branch tube which the thickness becomes thinner and thinner. While, the bigger h_1 will provide a longer time of balance force against the bulging to suppress the wall thinning. At the same time, the increase of the branch height is also suppressed. The height of T-tube branch was measured by the same method according to and the measurement data of wall thickness were listed in Fig.24.

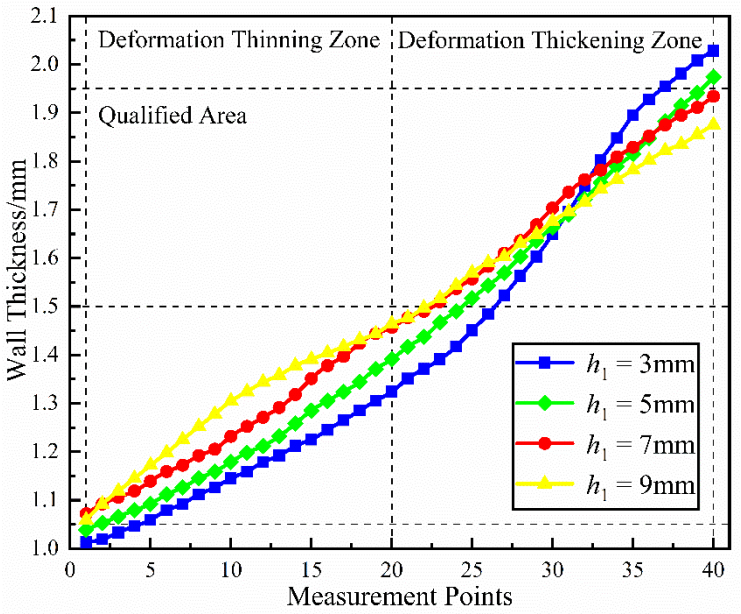

(a) Longitudinal Cross Section

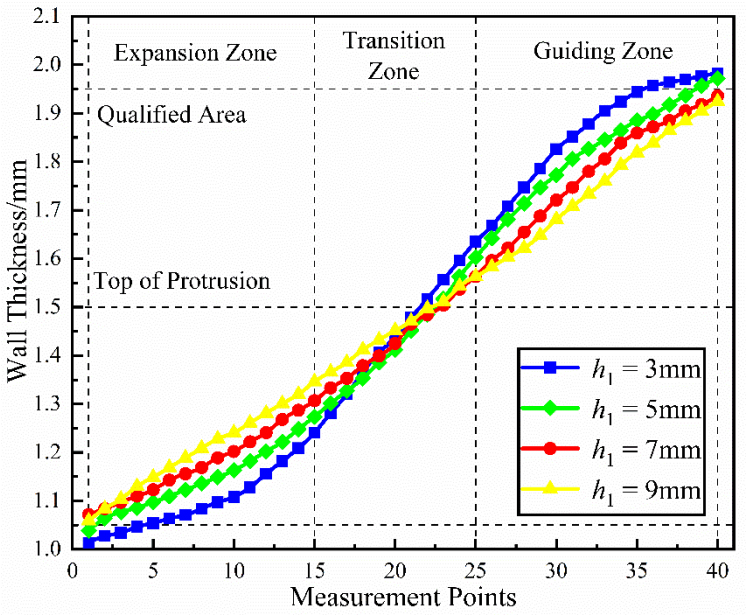

(b) Horizontal Cross Section

Fig.24. Wall Thickness Distribution of Cross Section of T-shaped Tube Formed by Different Reverse Height h_1 in Experiments

It can be found that when h_1 is less than 7mm, the wall thickness of the T-tube blank exceeds the safe area due to not enough balancing force provided. On the other hand, when h_1 is greater than 7mm, the position-limited back pressure mechanism will hinder the metal bulging one at an earlier time. Therefore, the wall thickness distribution was in the reasonable range when h_1 is 7mm and 9 mm, and the height of branch under the condition of h_1=7mm is larger than h_1=9mm, so the reverse height h_1=7mm is the best in experiment of T-tube bulging forming.

4.2.1 Effect of Load Path (MRRHAF)

In experiments, three different hardness (60HA, 75HA and 90HA) of polyurethane rubber rod were adopt. According to the simulation, the feed of axial punch Δl were set 23mm, 24mm and 25mm respectively, and the other corresponding process parameters remain unchanged and different load paths (MRRHAF) were tested. The T-shaped tube formed by different load paths (MRRHAF) as shown in **Error! Reference source not found.**.

(1) 60HA Δl=23mm

(2) 75HA Δl=23mm

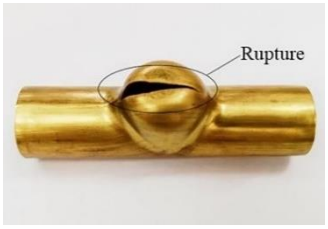

(3) 90HAΔl=23mm

(4) 60HA Δl=24mm

(5) 75HAΔl=24mm

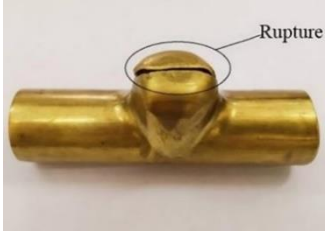

(6) 90HAΔl=24mm

(7) 60HA Δ*l*=25mm

(8) 75HAΔ*l*=25mm

(9) 90HAΔ*l*=25mm

Fig.25. Photograph of T-shaped Tube Formed by Different Load Paths (MRRHAF) in Experiments

The height of branch and the wall thickness distribution were measured from **Error! Reference source not found.** and listed in Table 4.

Table 4. Experiments Results of Different Load Path (MRRHAF)

Number	Rubber Hardness	Feed Δ*l* /mm	Height *h*/mm	Thickness (Max)/mm	Thickness (Min)/mm
1	60HA	23	15.1	1.932	1.056
2	75HA	23	15.8	1.938	1.042
3	90HA	23	16.2	1.942	0.998
4	60HA	24	16.1	1.934	1.053
5	75HA	24	16.9	1.943	1.059
6	90HA	24	17.1	1.974	1.014
7	60HA	25	13.2	2.015	1.109
8	75HA	25	15.1	1.985	0.994
9	90HA	25	17.5	1.974	1.015

According to Table 4, the following conclusions can be obtained from the experiments:

(1) When rubber hardness is 60HA and Δ*l* is 23mm, the shape of branch is similar to a convex hull and asymmetrical, and the height of branch is only 15.1mm which is a little hard to process further.

(2) When rubber hardness is 75HA and Δ*l* is 23mm, the quality of branch formed is better than before without obvious failure and the surface quality of T-shaped tube satisfies the forming requirements to be adopted.

(3) When rubber hardness is 90HA and Δ*l* is 23mm, the wall thickness thinning rate on the top of branch is too large so that the top of branch ruptured because of the hardness of rubber is too large, so it is unqualified.

(4) When rubber hardness is 60HA and Δ*l* is 24mm, the T-shaped tube satisfies the bulging forming requirements without failure and the height of branch is 16.1mm.

(5) When rubber hardness is 75HA and Δ*l* is 24mm, the quality of branch satisfies the forming requirements and the height of branch reaches 16.9mm.

(6) When rubber hardness is 90HA and Δ*l* is 24mm, the top of T-tube branch also ruptured but it is a little better than the forming result of (3).

(7) When rubber hardness is 60HA and Δ*l* is 25mm, it can be seen that because of the feed is too large, the materials of tube accumulate seriously to wrinkle which damage the rubber rod in tube.

(8) When rubber hardness is 75HA and Δl is 25mm, the tube also wrinkled but with the increase of hardness of rubber rod the wrinkle condition improved better than before, the rubber rod can be taken out from the tube easier than before.

(9) When rubber hardness is 90HA and Δl is 25mm, the height of branch reaches 17.5mm which is largest of nine experiments without failure.

It can be also found from Table 4 that the simulation results are in accord with the experimental results. According to the requirements of the wall thickness thickening rate and thinning rate, there are three experiments ((1), (4), and (5)) satisfy the forming requirements. The wall thickness distribution of (1), (4) and (5) were measured and shown in Fig.26.

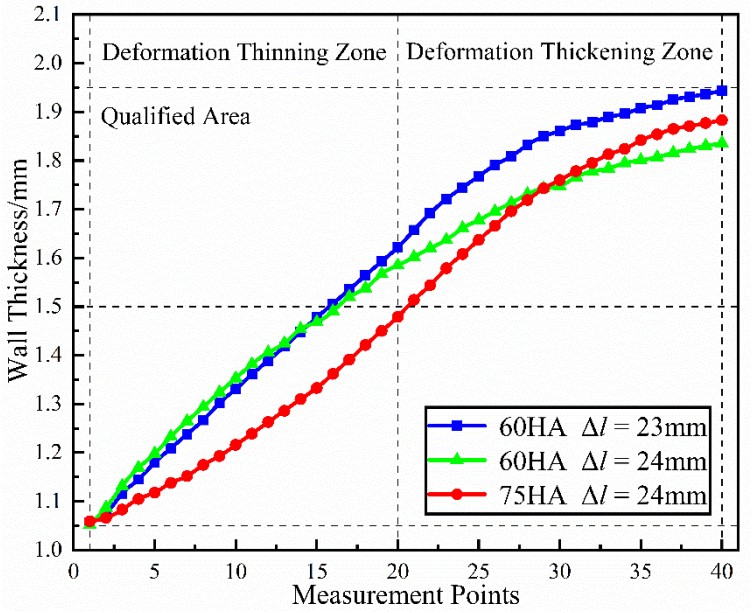

(a) Longitudinal Cross Section

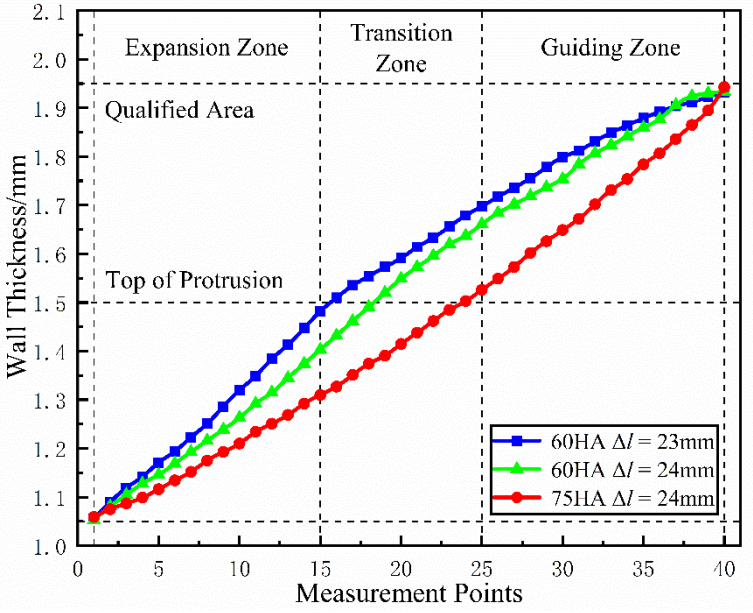

(b) Horizontal Cross Section

Fig.26. Wall Thickness Distribution of Cross Section of T-shaped Tube Formed by Different Load Paths (MRRHAF) in Experiments

The Fig.26 shows the wall thickness distribution of the three conditions, the working condition

(1), (4) and (5) conforms to the safety and qualified area, under the premise of meeting the production conditions, the workpiece with the highest branch height is conductive to subsequent machining, the working condition (5) with the branch height of 16.9mm is considered the best result in experiments.

The relationship between feed, rubber hardness and height of branch during T-shaped tube bulging forming experiments with polyurethane rubber rod can be showed in Fig.27.

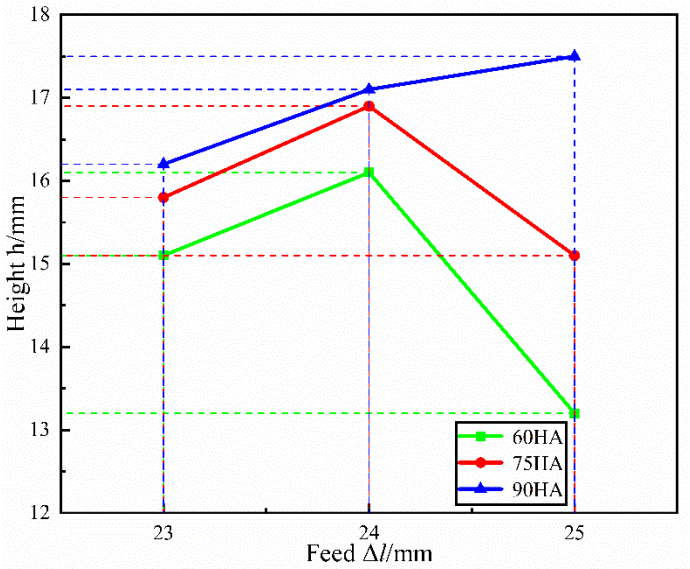

Fig.27. Relationship Between Rubber Hardness, Feed and Forming Height

It can be seen from Fig.27 that when rubber hardness is fixed at 90HA, too small feed cannot reach the strength of material compensation, so that the pressure inside the tube increases too fast and branch tube breaks due to insufficient material compensation. When rubber hardness is fixed at 60HA, excessive feed is not conducive to material flow and accumulates at the transition fillet, buckling and wrinkling occur to it which both affect subsequent use. To sum up, larger (smaller) rubber hardness increases (decreases) the friction between the tube and the cavity of the die, on this basis, increasing the appropriate feed can obtain a T-tube with a larger branch height in the qualified area. When axial feed is fixed, the greater rubber hardness and force push the metal to transfer into the branch tube with the increase of rubber hardness, so more and more material is demanded with the increase of the branch tube. However, not enough metal is supplemented into the branch tube due to the greater friction resistance. Therefore, the thinnest part of the tube wall becomes thinner and more uneven and even breaks, such as working condition (3) and (6) in **Error! Reference source not found.**. Therefore, only when the feed is matched with the rubber hardness reasonably can the wall thickness be evenly distributed. In this experiment, the best matching relationship of load path is that rubber hardness is 75HA and feed Δl is 24mm.

5 Discussions and Conclusions

In this study, the rubber flexible-die compound bulging forming method was developed to achieve T-shaped tube with small radius and thin wall by FEM and experiments. The effects of three key factors over the forming limitation (forming height of T-shaped tube branch) and the wall thickness distribution are investigated. The main conclusions are achieved as follows:

(1) A new position-limited back pressure mechanism was designed in study which is made up with rigid position-limited lever, flexible back pressure medium and rigid spacer. Compared with

traditional back pressure device, it can control the time when the back force is added to the tube by adjusting reverse height and length of flexible back pressure medium and decrease experimental cost. The back pressure is changeable with the compression of flexible back pressure medium rather than fixed which is better to improve forming limitation and make wall thickness distribution more uniform to suppress rupturing at the top of branch.

(2) The finite element model for rubber compound bulging forming is established and the accuracy of the finite element model is verified by the forming experiment. Both the forming limitation and the wall thickness distribution between the simulations and experiments agree well to each other with maximum deviation about 5%.

(3) Aiming at the influence of punch front distance l_1, the l_1 is set 3.5mm, 5mm and 6.5mm respectively. The height of T-shaped tube branch increases with the increase of punch front distance l_1, the height of branch reaches the highest when l_1 is 6.5mm. The thinning rate of the wall thickness at the branch decreases first and then increases, the thickening rate at the transition fillet gradually decreases and the difference of wall thickness increases gradually. When l_1 is 6.5mm the maximum thinning rate and thickening rate are more than 30%. When the l_1 is 5mm, the branch of T-shaped reaches the highest both in simulation and experiments under the requirements of thinning rate and thickening rate.

(4) Aiming at the influence of reverse height h_1, the h_1 is set 3mm, 5mm, 7mm and 9mm respectively. Both in simulation and experiments, with the increase of reverse height h_1 the height of branch h increases first and then decreases, when h_1 is 5mm the height of branch reaches highest. The maximum wall thickness decreases and the minimum wall thickness increases with the increase of reverse height h_1, the bigger h_1 is beneficial to the wall thickness thinning suppresses at the top of branch. When h_1 is 7mm, the branch of T-shaped reaches the highest both in simulation and experiments with best parameter of reverse height.

(5) Aiming at the influence of load path (matching relationship between rubber hardness and axial feed), the rubber hardness is set 60HA, 70HA and 90HA and the axial feed Δl is set 23mm, 24mm and 25mm respectively. The rubber hardness is an important factor to affect the wall thickness distribution without excessive wall thickening and thinning, in experiments, the larger hardness of rubber can cause rupturing at the top of branch and the lower cause wrinkling of the tube. When rubber hardness is fixed, with the increase of feed the difference of wall thickness increases. When axial feed is fixed, the height of branch increases with the increase of rubber hardness and internal pressure. The best matching relationship is the rubber hardness of 75HA and the feed Δl of 24mm both in simulation and experiments.

In conclusion, when the punch front distance l_1 is 5mm, reverse height h_1 is 7mm, rubber hardness is 75HA, and the axial feed Δl is 24mm, the T-shaped tube branch reaches the highest and the maximum forming limitation with the most uniform wall thickness.

Acknowledgements

This work was financially supported by the Natural Science Foundation of Liaoning Province, China (No. 2019ZD0240). The authors wish to express their gratitude.

Declarations

Funding

This work was financially supported by the Natural Science Foundation of Liaoning Province, China (No. 2019ZD0240).

Conflicts of interest/Competing interests

No conflict of interest exists in the submission of this manuscript.

Availability of data and material (data transparency)

Not applicable

Code availability (software application or custom code)

Not applicable

Authors' contributions

The first author (corresponding author) is the supervisor teacher and helped design the experiments and provided the experiment setups.

The second author designed and conducted the experiments and wrote the paper.

The fourth author provided financial supports and suggestions in experiments.

The third and fifth authors helped with the experiments.

Additional declarations for articles in life science journals that report the results of studies involving humans and/or animals

Not applicable

Ethics approval (include appropriate approvals or waivers)

The work was original research that has not been published previously, and not under consideration for publication elsewhere, in whole or in part.

Consent to participate (include appropriate statements)

The authors all approved to participate.

Consent for publication (include appropriate statements)

It is approved by all authors for publication

References

[1] Vakili-Tahami F, Majnoun P, Ziaei-Asl A (2019) Controlling the in-service welding parameters for T-shape steel pipes using neural network. International Journal of Pressure Vessels and Piping 175: 103937.
[2] Dong G J, Bi J, Du B, Chen X H, Zhao C C (2017) Research on AA6061 tubular components prepared by combined technology of heat treatment and internal high pressure forming. Journal of Materials Processing Technology 242:126-138.
[3] Wang H F (2004) Forming Study and Process Control of the Multi-tube's Hydroforming. Northwestern Polytechnical University.
[4] Dond S K, Kolge T, Choudhary H, Sharma A, Dey G-K (2020) Determination of magnetic coupling and its influence on the electromagnetic tube forming and discharge circuit parameters. Journal of Manufacturing Processes 54:19-27.
[5] Lv H J, Wang Q (2000) Processing technology and profile controlling of free electromagnetic bulging for LF3 Al alloy tube. Journal of Aerospace Materials Technology 3: 49-52.
[6] Trana K (2002) Finite element simulation of the tube hydroforming process-bending performing and hydroforming. Journal of Materials Processing Technology 127(3): 401-408.
[7] Ray P, Mac Donald B J (2005) Experimental study and finite element analysis of simple X- and T-branch tube hydroforming processes. International Journal of Mechanical Sciences 47: 1498-1518.
[8] Feng Y Y, Zhang H G, Luo Z A, Wu Q L (2019) Loading path optimization of T tube in hydroforming process using response surface method. The International Journal of Advanced Manufacturing Technology 101: 1979-1995.
[9] Nikhare C, Weiss M. Hodgson P D (2017) Buckling in low pressure tube hydroforming. Journal of Manufacturing Processes 28:1-10.
[10] Nakamori T, Shukuno K, Manabe K (2017) In-process controlled Y-shape tube hydroforming with high accurate built-in sensors. Procedia Engineering 184: 43-49.
[11] Dai L F (2018) Study on the influence factors of Hydroforming of 5A02 aluminum alloy Reducer Tee. Nanchang Hangkong University.
[12] Chen Z Z, Liu B (2011) Simulation of Compound bulging process for T-branch tubes using rubber medium. Advanced Materials Research 228-229: 88-95.
[13] Wang P Y (2016) Research on magnetorheological flexible-die forming technology and forming limit for Al1060 sheet. Harbin Institute of Technology.
[14] Zhang F F, Wei Y Y, He K, Hang Z Q (2020) Experimental investigation on electro-hydraulic forming with flexible-die. Procedia Manufacturing 50: 324-327.
[15] Girard A C, Grenier Y J, Donald B J M (2006) Numerical simulation of axisymmetric tube bulging using a urethane rod. Journal of Materials Processing Technology 172(3): 346~355.
[16] Omid S and Ghader F (2016) Rubber pad tube straining as a new severe plastic deformation method for thin-walled cylindrical tubes. Proceedings of the Institution of Mechanical Engineers, Part B: Journal of engineering manufacture 230(10): 1845-1854.
[17] Chen Z Z and Liu B (2011) Simulation of bulge forming process for three-way tube using rubber medium. Journal of Huaqiao University (Natural Science) 32:485-491.
[18] Zou Q S and Liu B (2013) Influence of mold structure parameters on T-shapes tubes by compound bulging using rubber medium. Journal of Huaqiao University (Natural Science) 34: 121-125.
[19] Wang Y, Nielsen K B, Lang L, Endelt B (2018) Investigation into bulging-pressing compound forming for sheet metal parts with very small radii[J]. The International Journal of Advanced Manufacturing Technology 95: 445-457.
[20] Kim B, Lee S B, Lee J, Cho S, Park H, Park YSH (2012) A comparison among Neo-Hookean

model, Mooney-Rivlin model, and Ogden model for chloroprene rubber[J]. International Journal of Precision Engineering and Manufacturing 13(5): 759-764.
[21] Zhang L, Li Z H and Ma X Q (2018) Study on parameter characteristics of rubber Mooney-rivlin model. Noise and vibration control 38: 427-430.
[22] Liu G, Xie W C, Yuan S J, Yao J Q, Miao Q B (2004) Internal high pressure forming of hollow part with a big section difference. Journal of Material Science and Technology 12(4): 398-401.
[23] Zhu S J, Li J, Lin X K, Chang X, Su H D, Wu L (2018) Simulation and optimization on hydroforming of T-shape tube based on orthogonal experiment. Forging and Stamping Technology 43(9):75-82.
[24] Li X M, Xia J Q, Hu G A (2002) Technology analysis and forming force calculation of compound forming of solid three-way tube. Metal-forming Machinery 4: 37-38.
[25] Yang Z Z, Wang G F, Liu Y L, Huang L, Nie X H, Xu Y, Zhao J L (2019) Correlation between processing technology and cross-sectional distortion of small-radius hot-bending. Oil & Gas Storage and Transportation 38(03): 338-344.
[26] Xu X B, Guan Q (2010) Numerical simulation of wall thickness change in tube bending. Forging and Stamping Technology 35(06): 133-136.

Figures

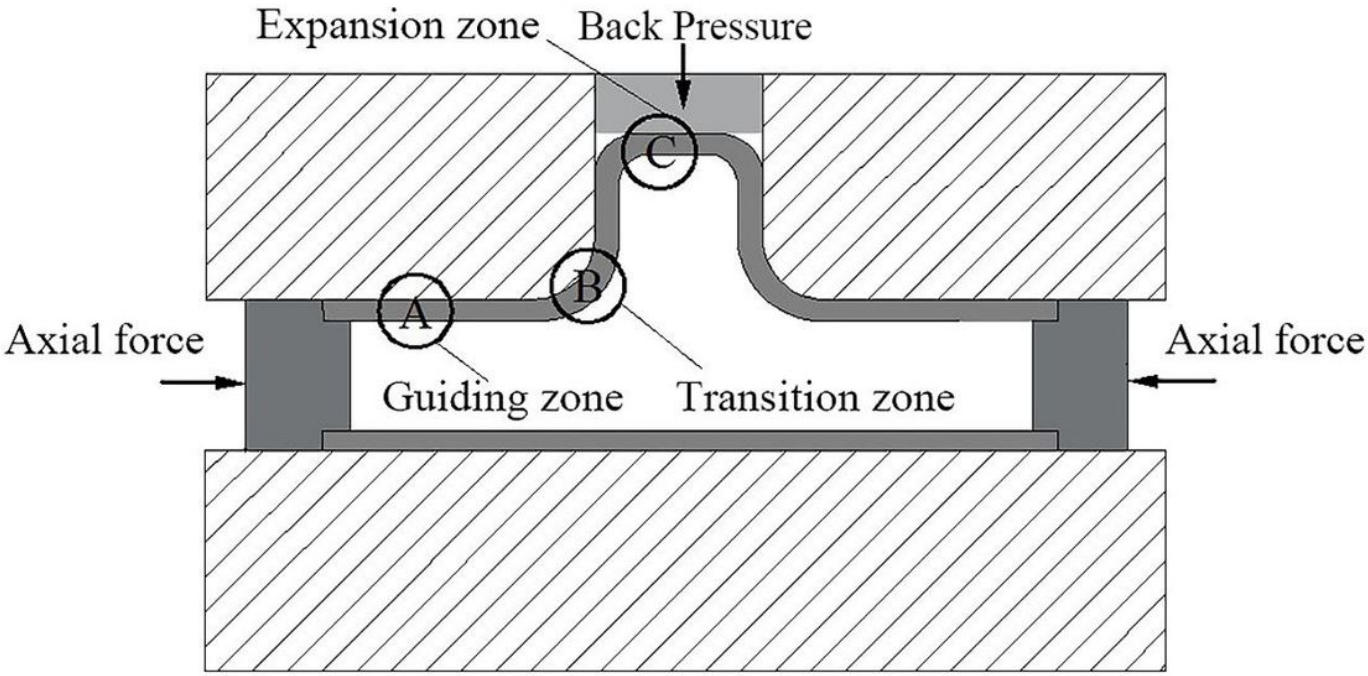

Figure 1

Principle of T-shaped Tube Compound Bulge Forming

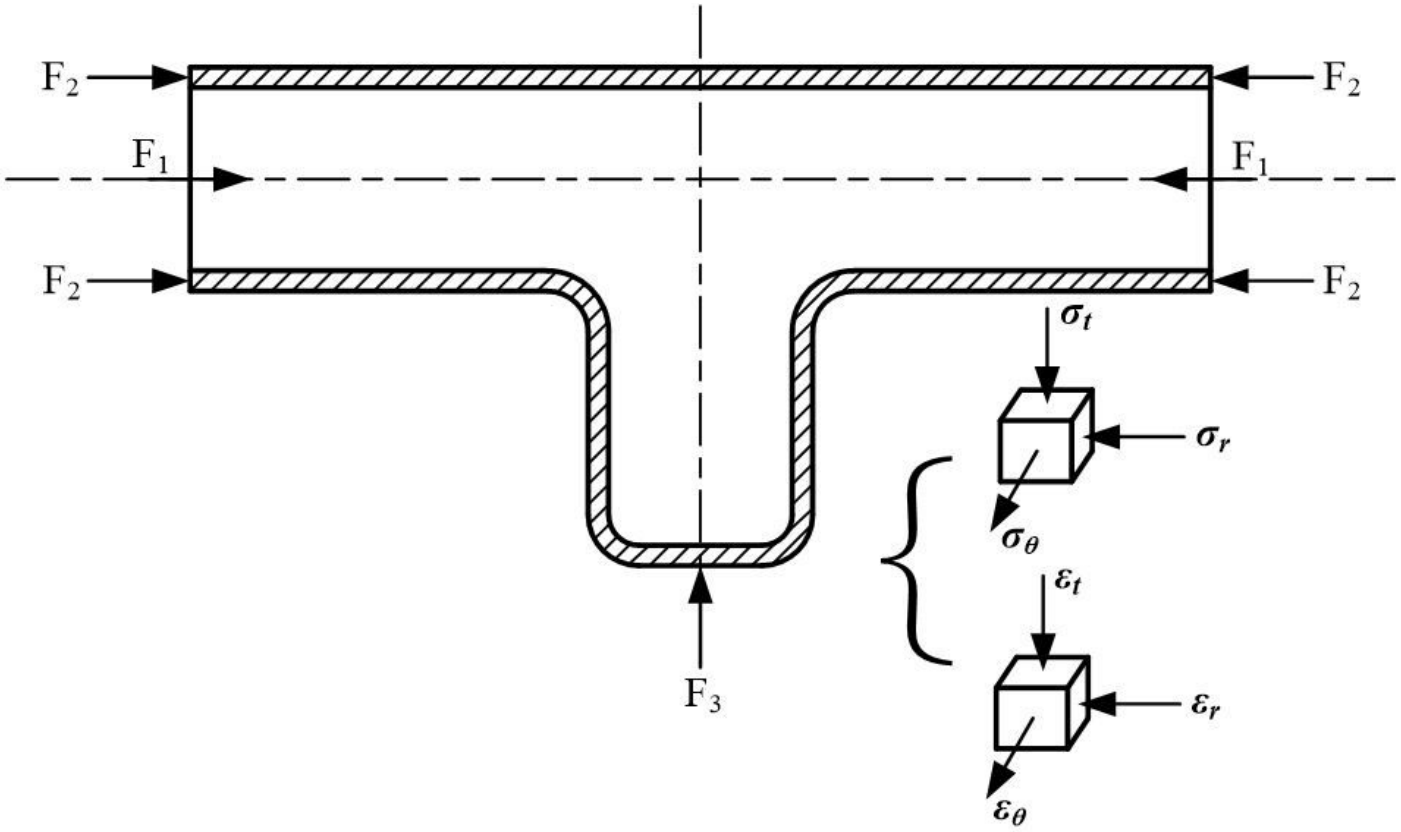

Figure 2

Compound Bulging Mechanical State

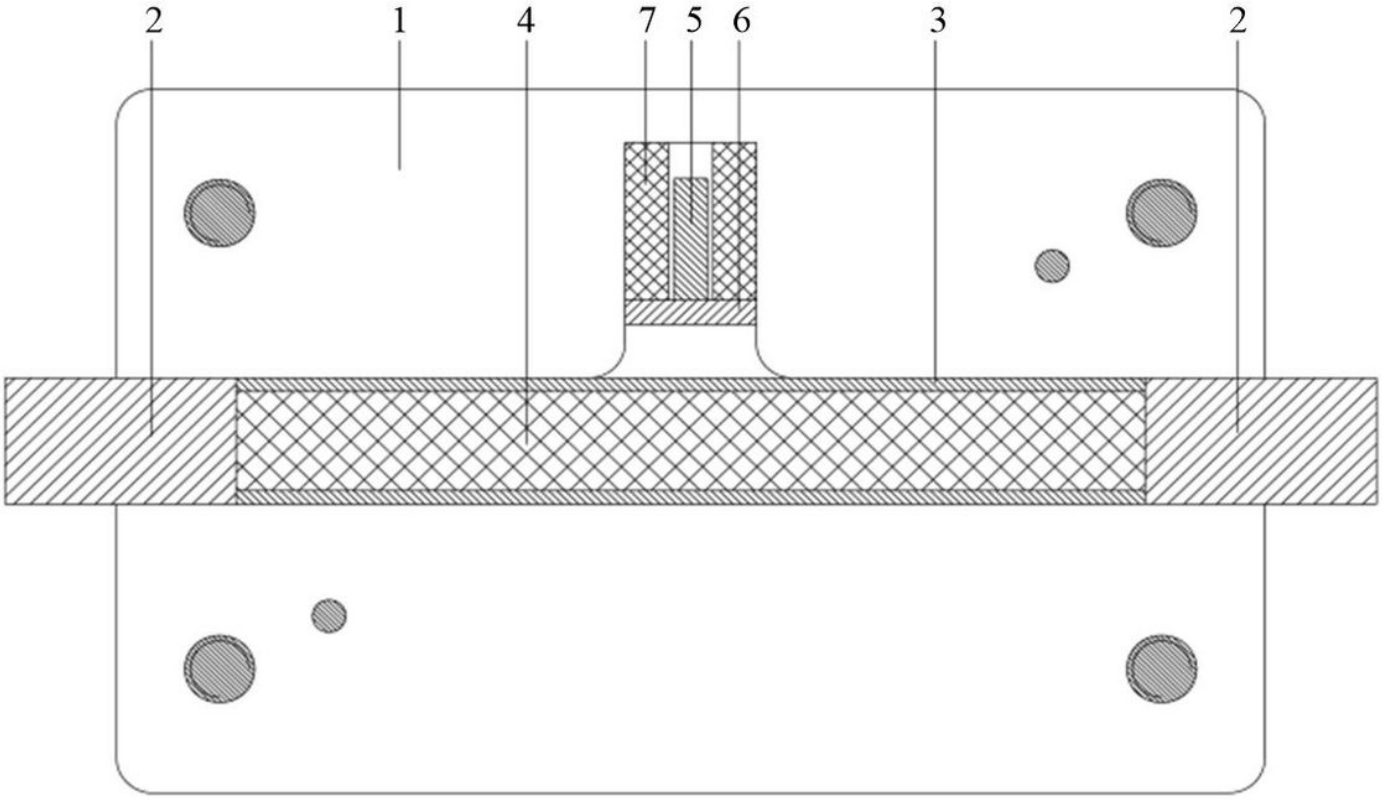

Figure 3

Compound Bulging Forming Mechanism of Original State

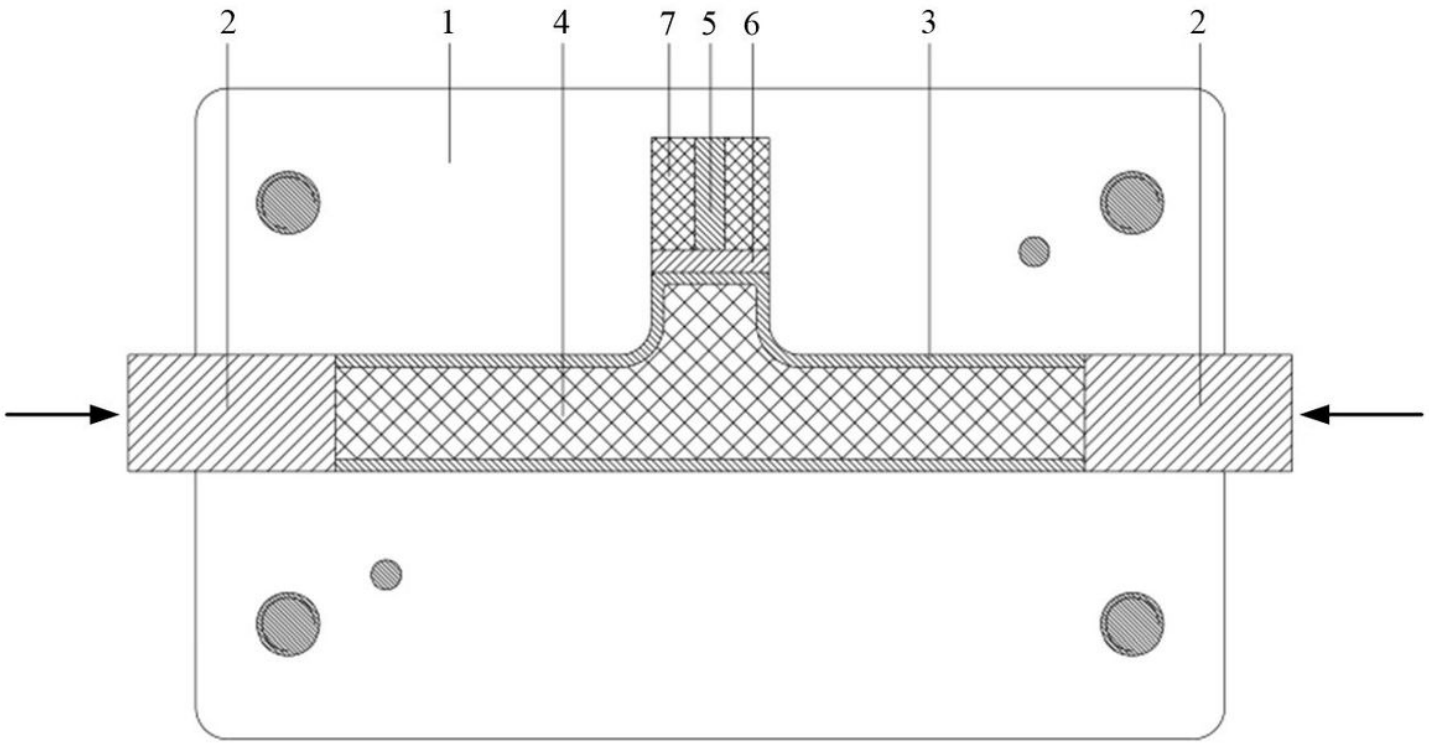

Figure 4

Compound Bulging Forming State After Forming

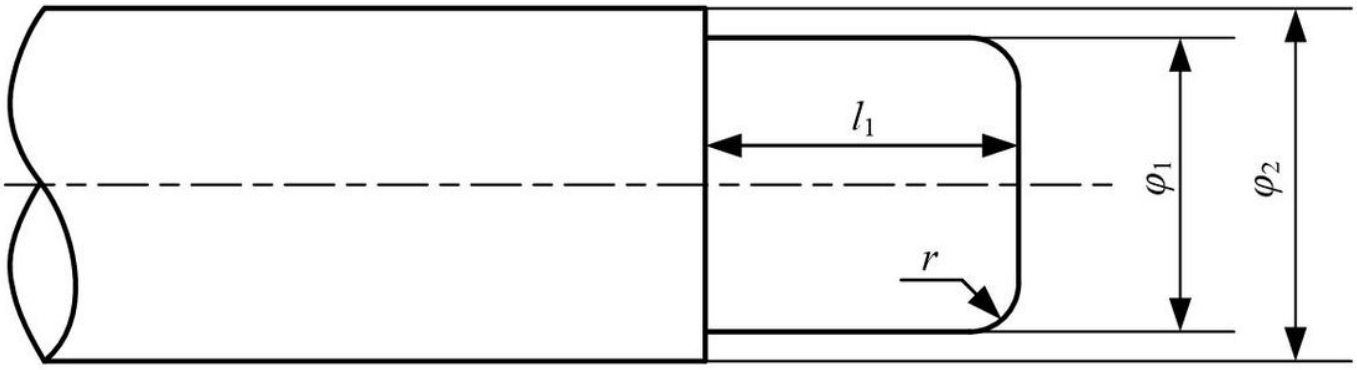

Figure 5

Schematic diagram of punch structure

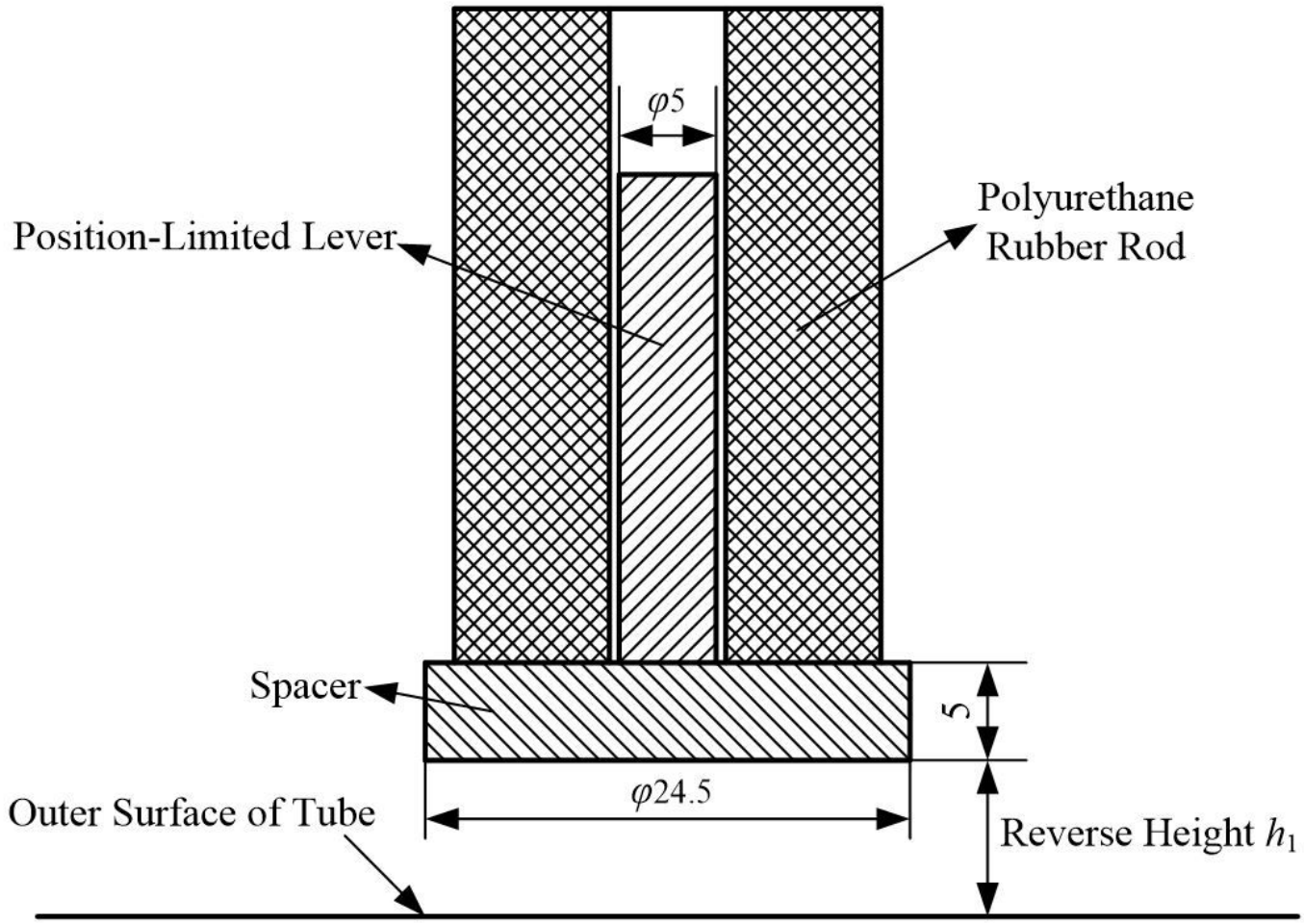

Figure 6

Schematic diagram of the position-limited back pressure mechanism

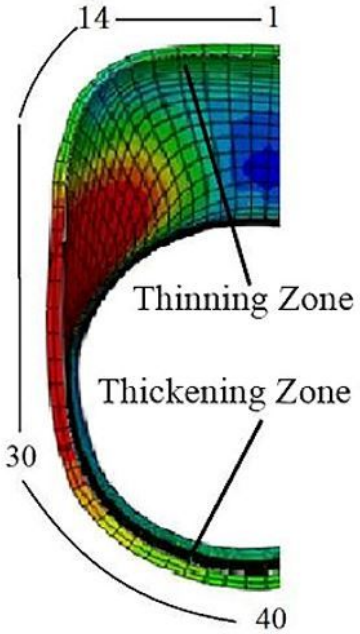

(b) Longitudinal Cross Section

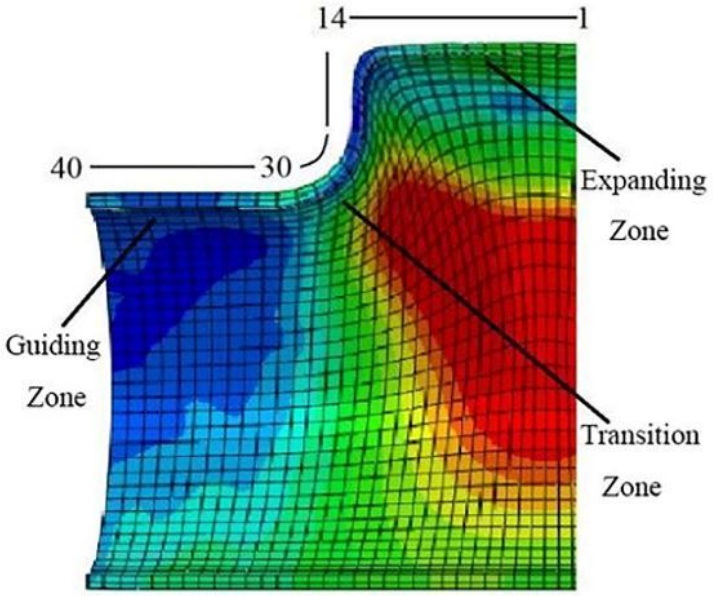

(c) Horizontal Cross Section

Figure 7

Cross Section of T-tube in Simulation

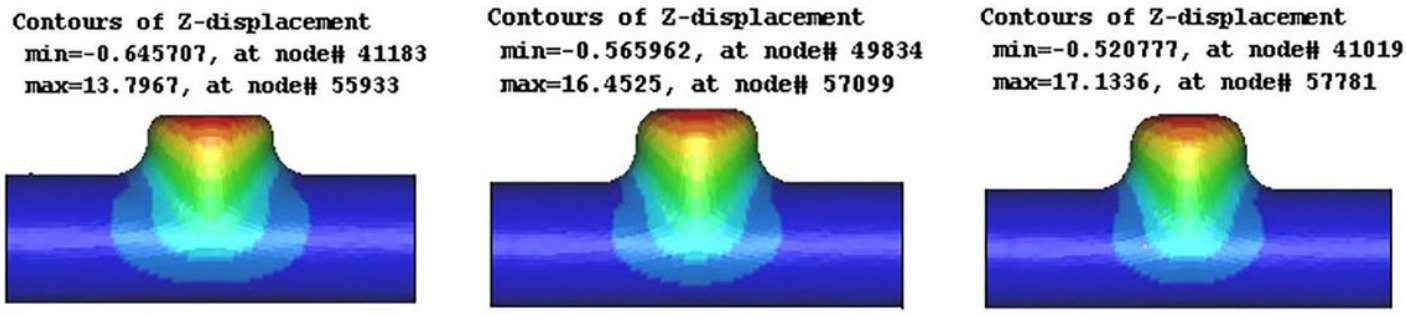

(a) l_1=3.5mm (b) l_1=5mm (c) l_1=6.5mm

Figure 8

Z-Displacement of T-shaped Tube Formed by Different Punch Front Distance l1 in Simulation

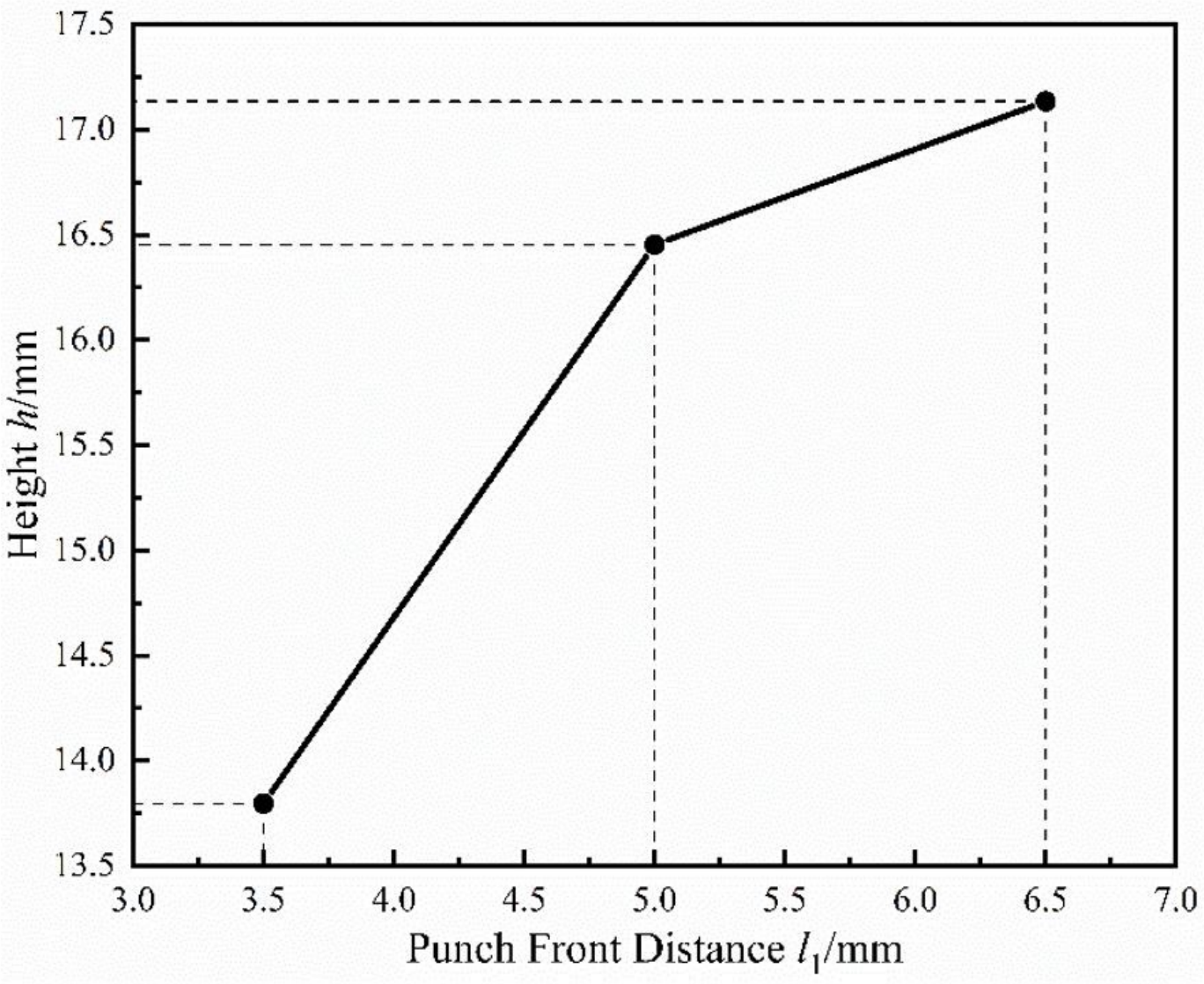

Figure 9

Height of T-shaped Tube Branch Formed by Different Punch Front Distances l1 in Simulation

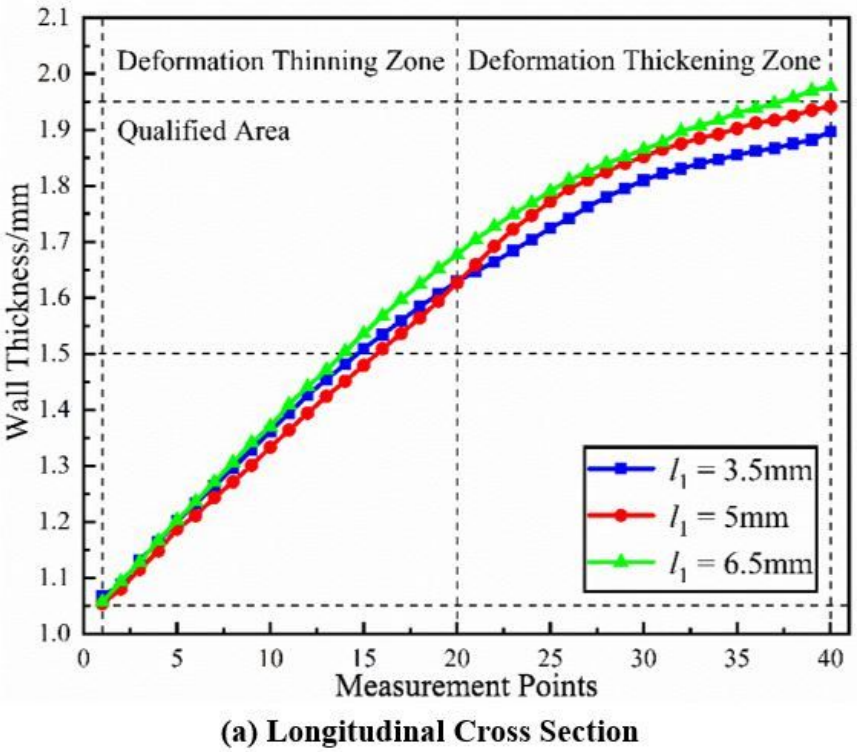

Figure 10

Wall Thickness Distribution of Cross Section of T-tube Formed by Different Punch Front Distance l1 in Simulation

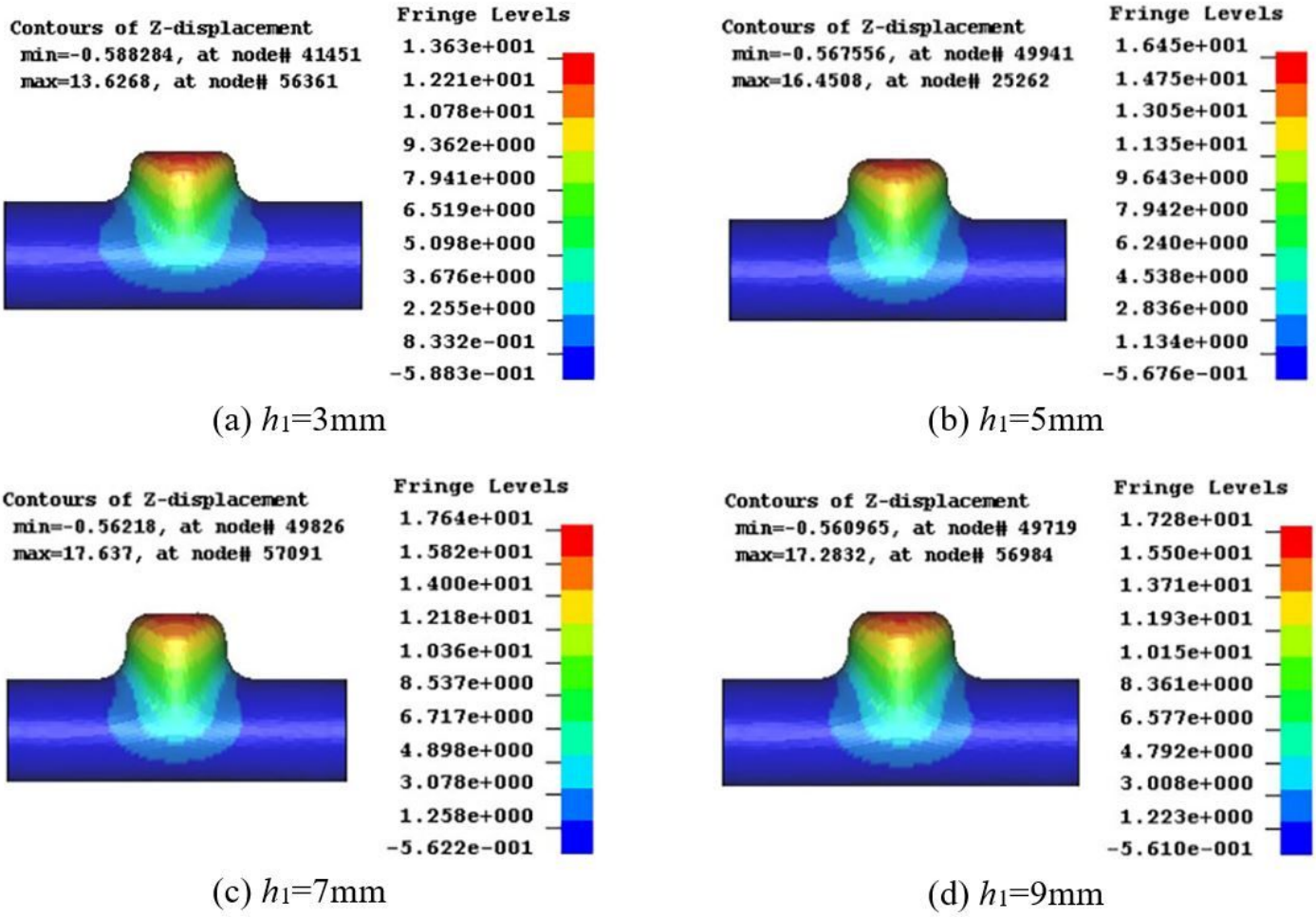

Figure 11

Z-Displacement of T-shaped Tube Formed by Different Reverse Height h1 in Simulation

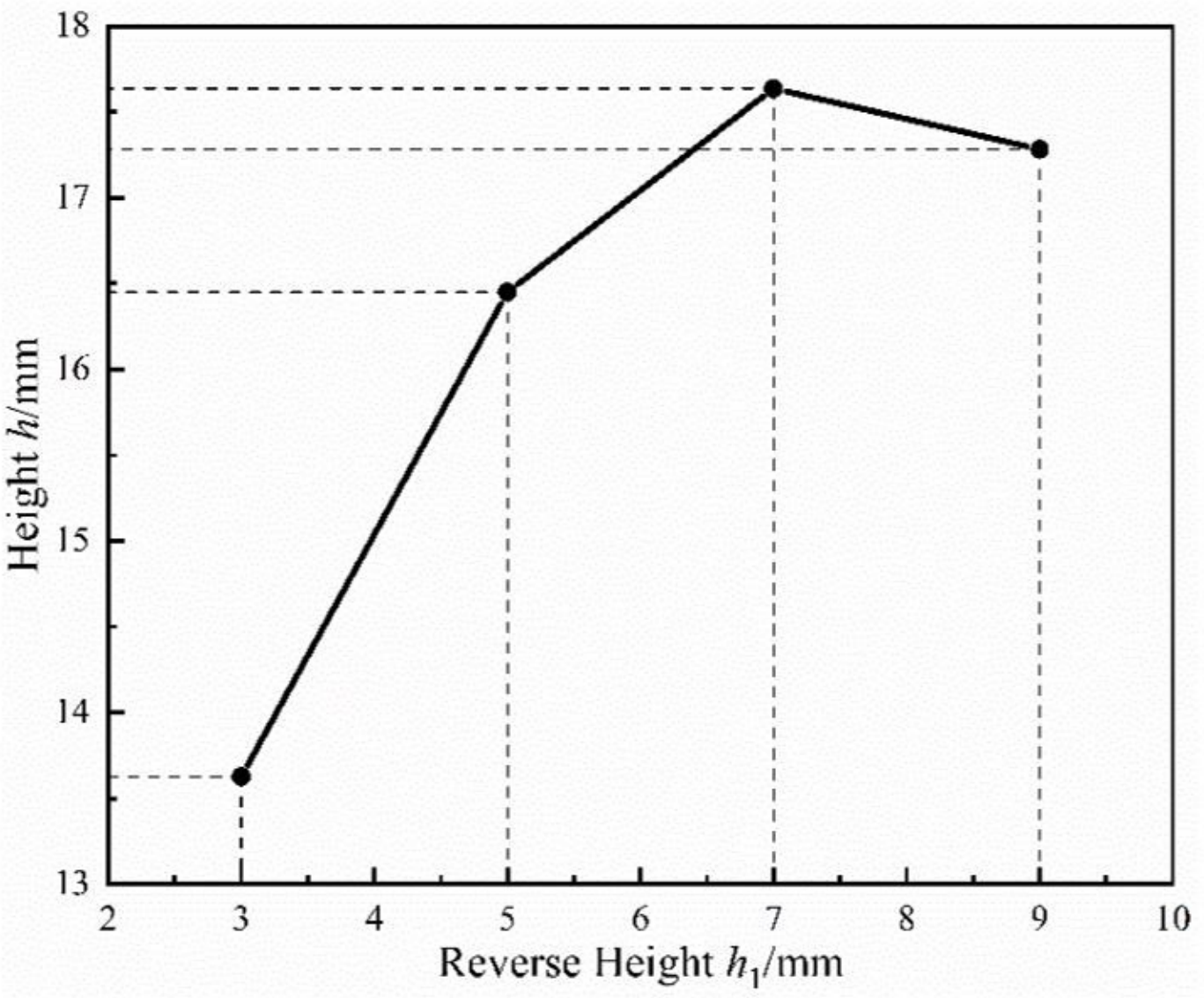

Figure 12

Height of T-shaped Tube Branch Formed by Different Reverse Height h1 in Simulation

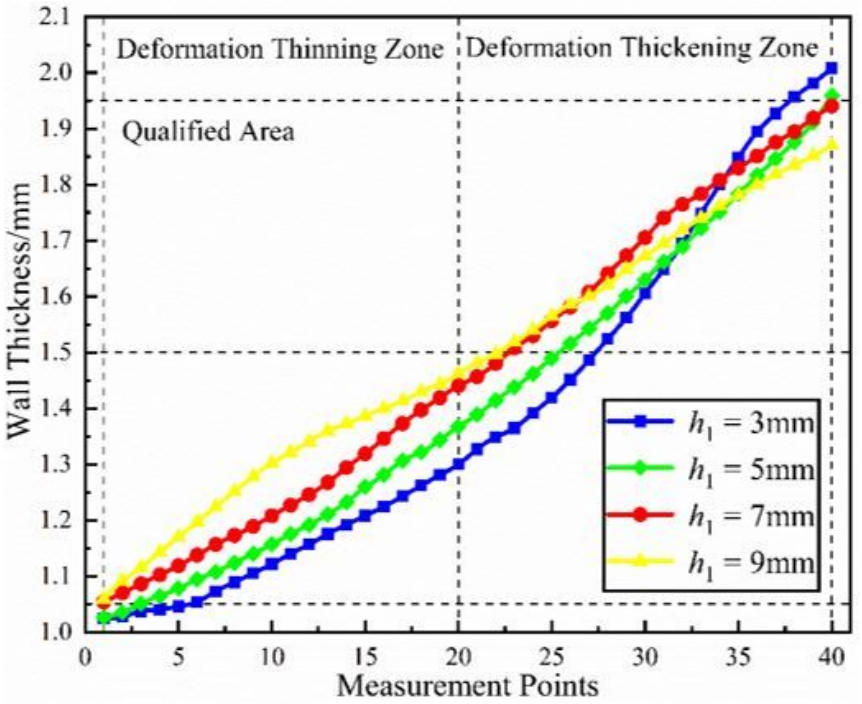

(a) Longitudinal Cross Section

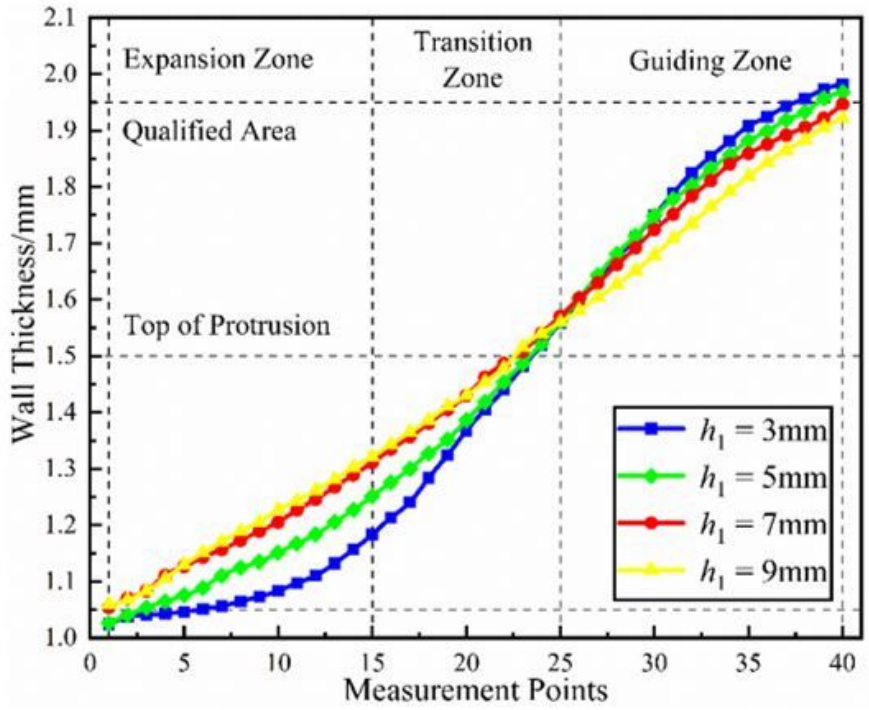

(b) Horizontal Cross Section

Figure 13

Wall Thickness Distribution of Cross Section of T-tube Formed by Different Reverse Height h1 in Simulation

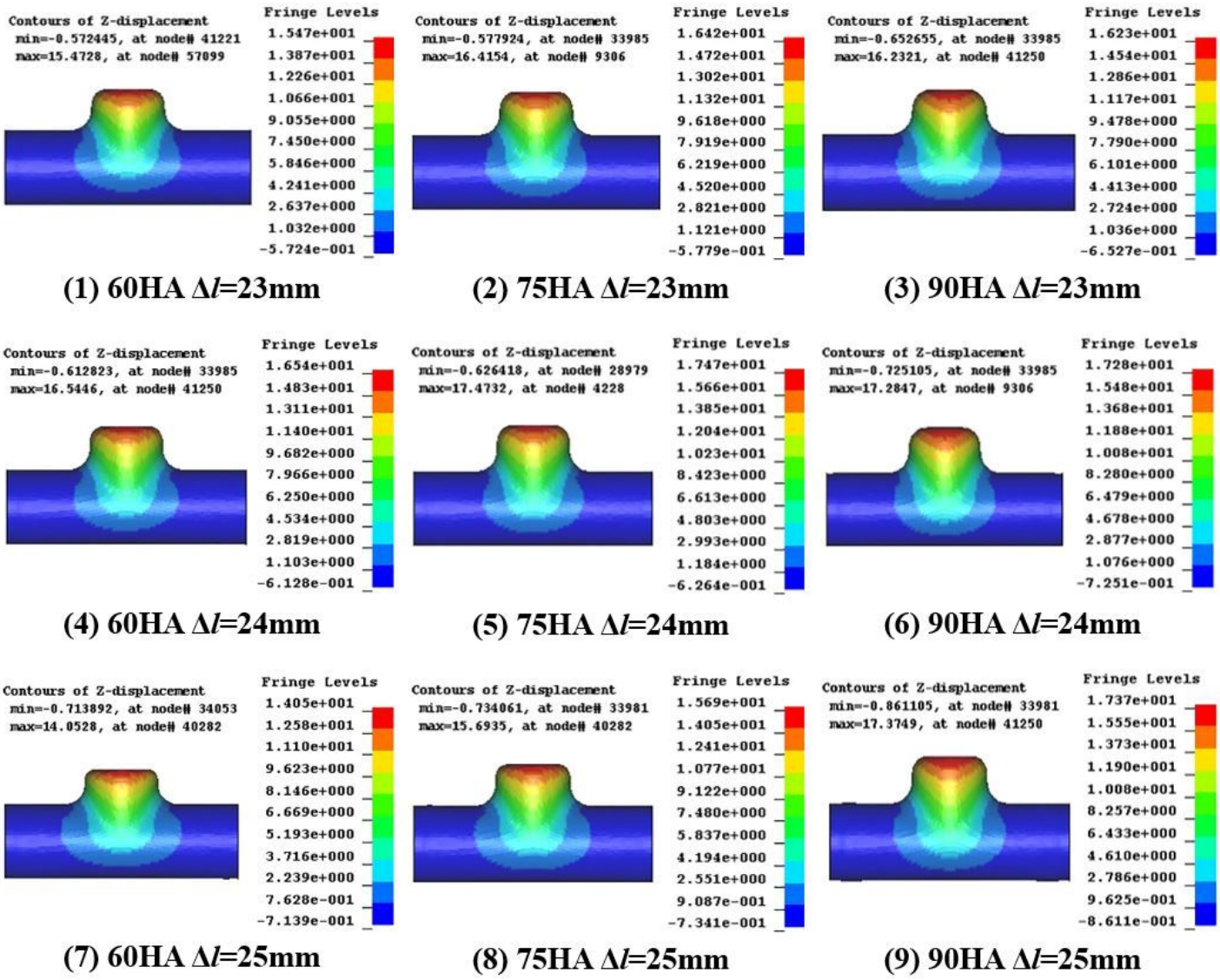

Figure 14

Z-Displacement of T-shaped Tube Formed by Different Load Path (MRRHAF) in Simulation

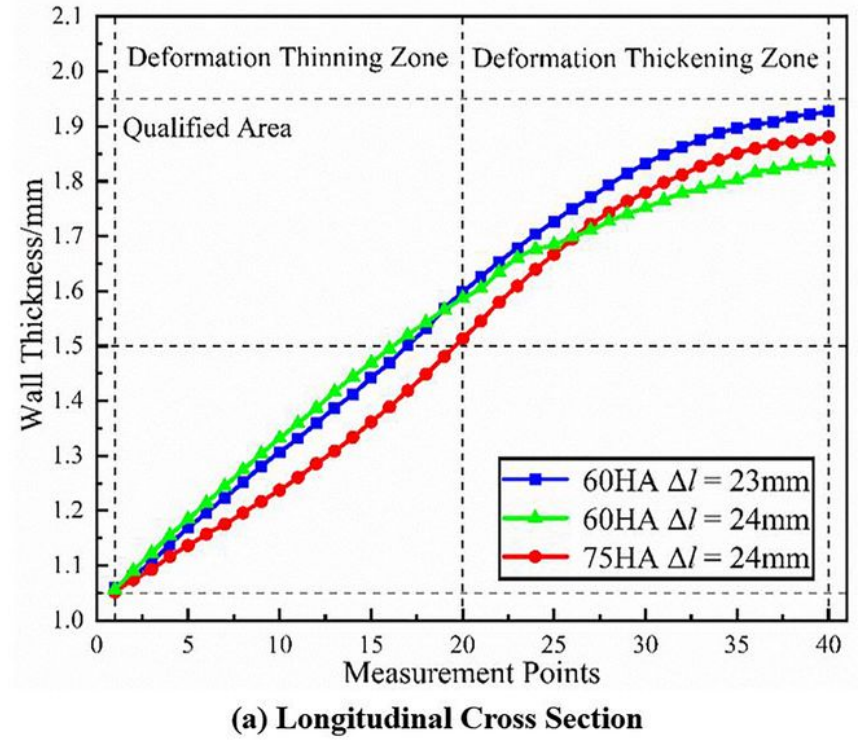

Figure 15

Wall Thickness Distribution of Cross Section of T-tube Formed by Different Load Paths (MRRHAF) in Simulation

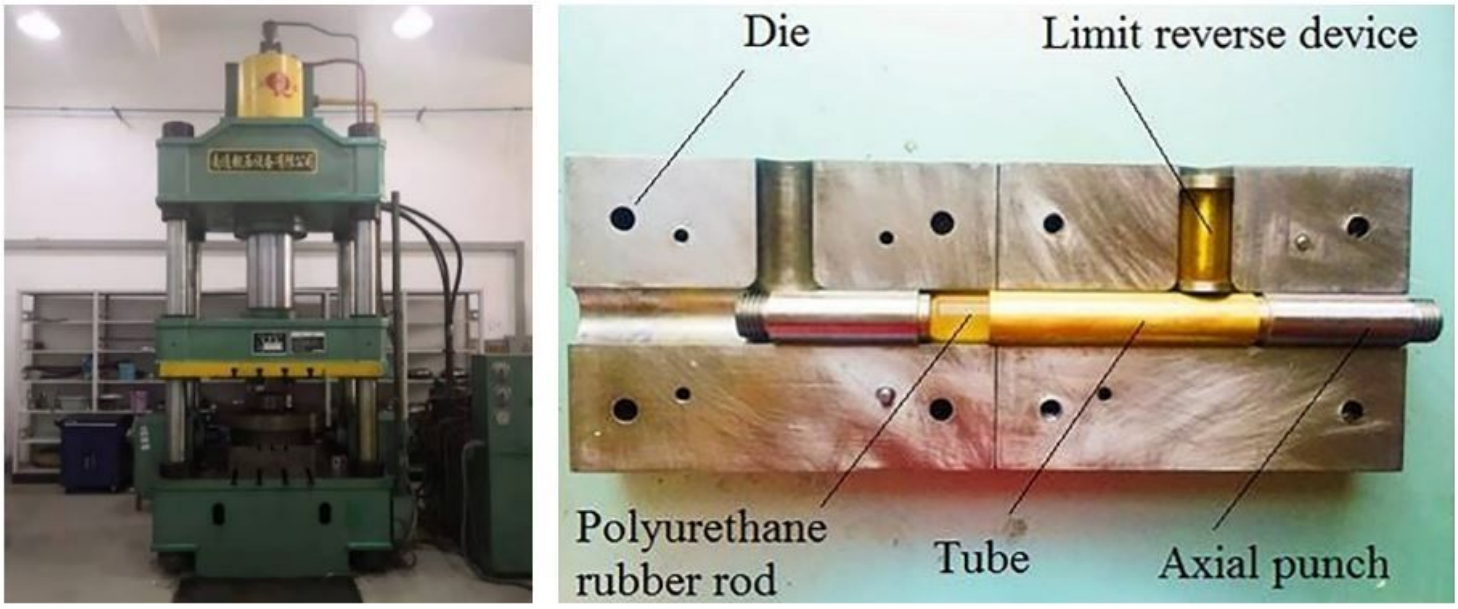

Figure 16

YQ32-400 Hydraulic Press and Forming Device

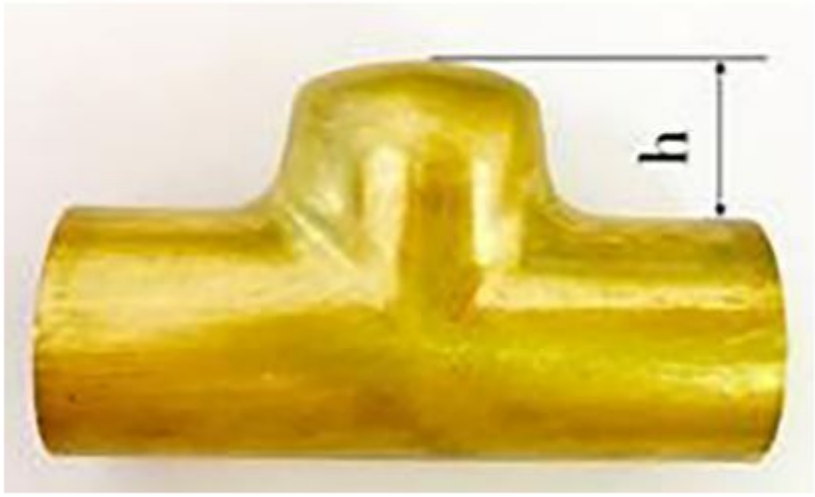

Figure 17

The Height h of T-tube Branch

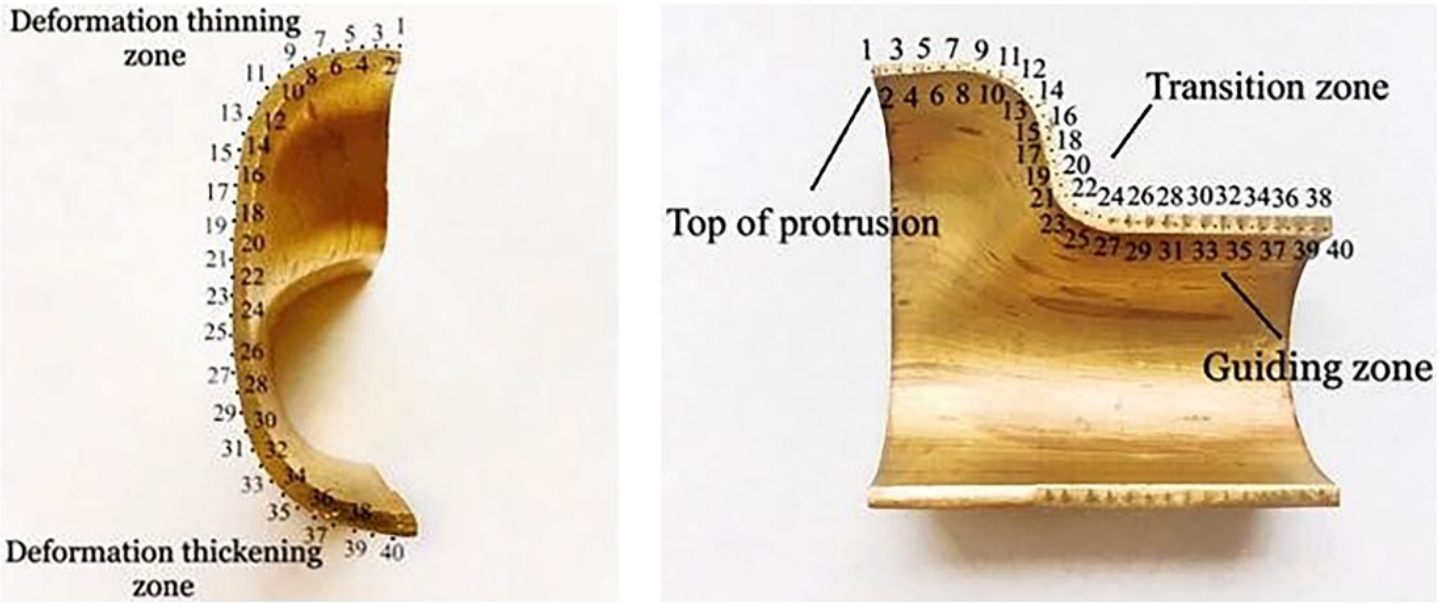

Figure 18

Cross section of T-shape tube: (a) Longitudinal cross section (b) Horizontal cross section

Figure 19

Photography of the T-shaped Tube Formed by Different Punch Front Distances l1

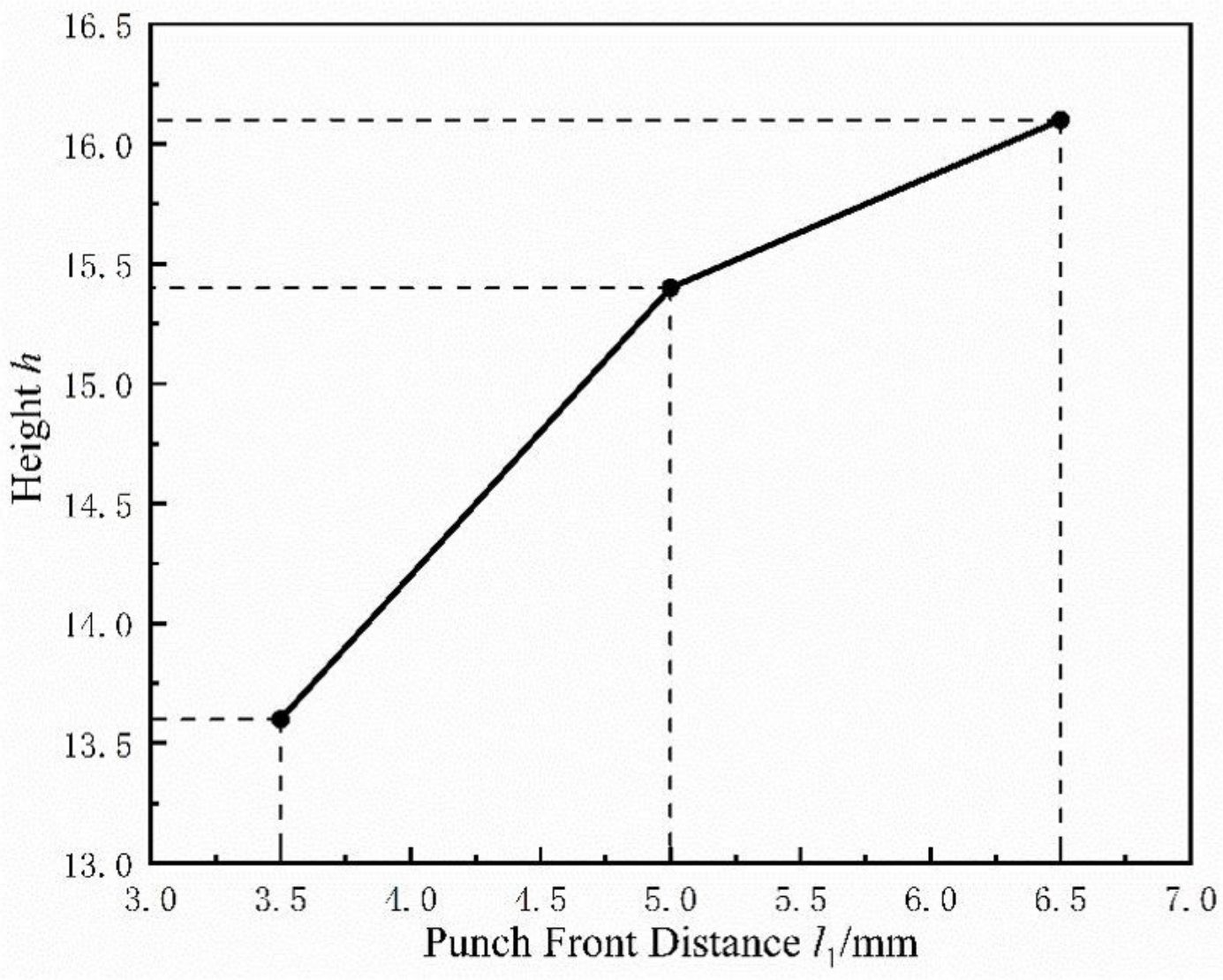

Figure 20

Height of T-shaped Tube Branch Formed by Different Punch Front Distances l1 in Experiments

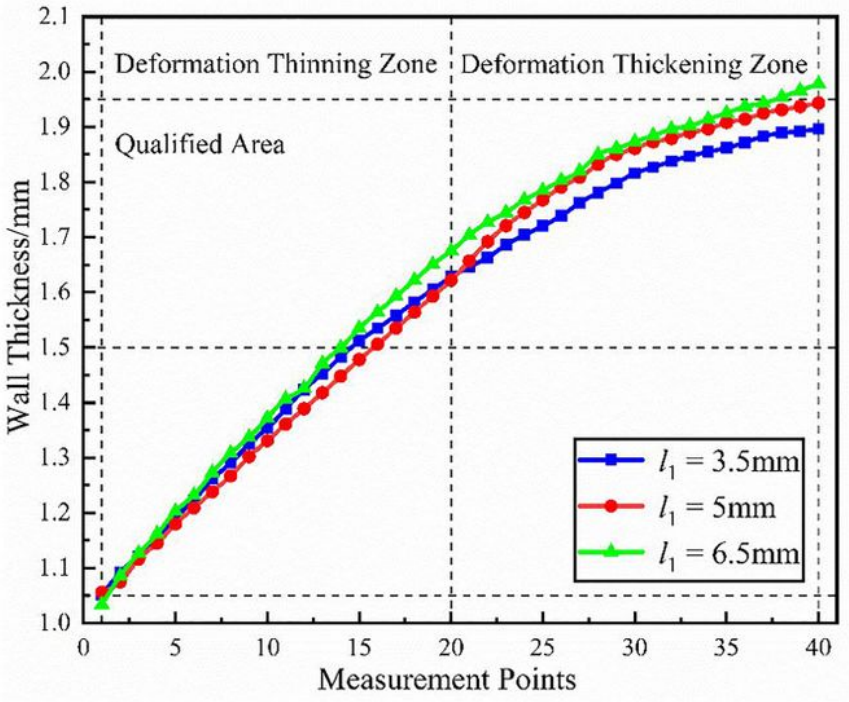

(a) Longitudinal Cross Section

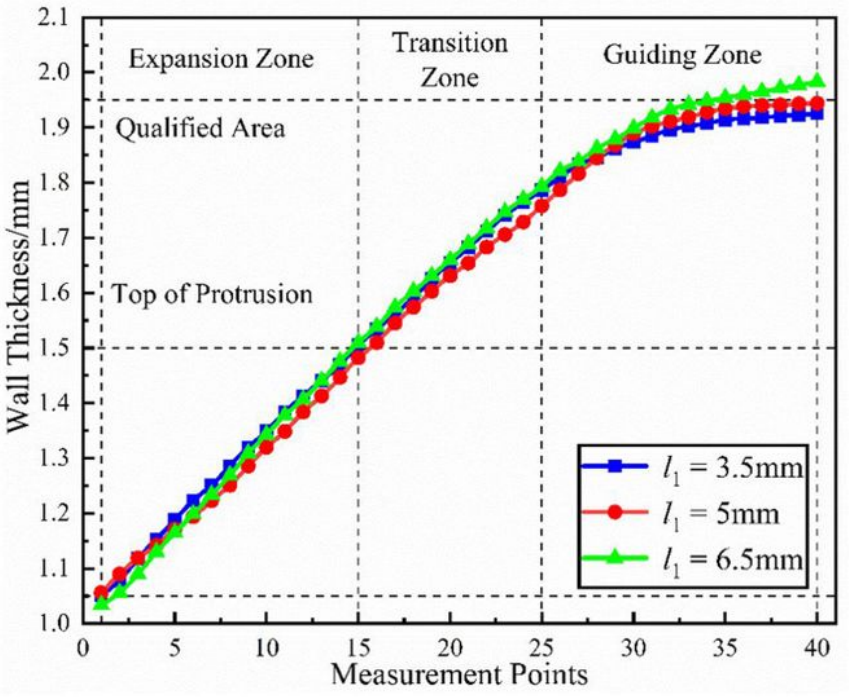

(b) Horizontal Cross Section

Figure 21

Wall Thickness Distribution of Cross Section of T-shaped Tube Formed by Different Punch Front Distances l1 in Experiments

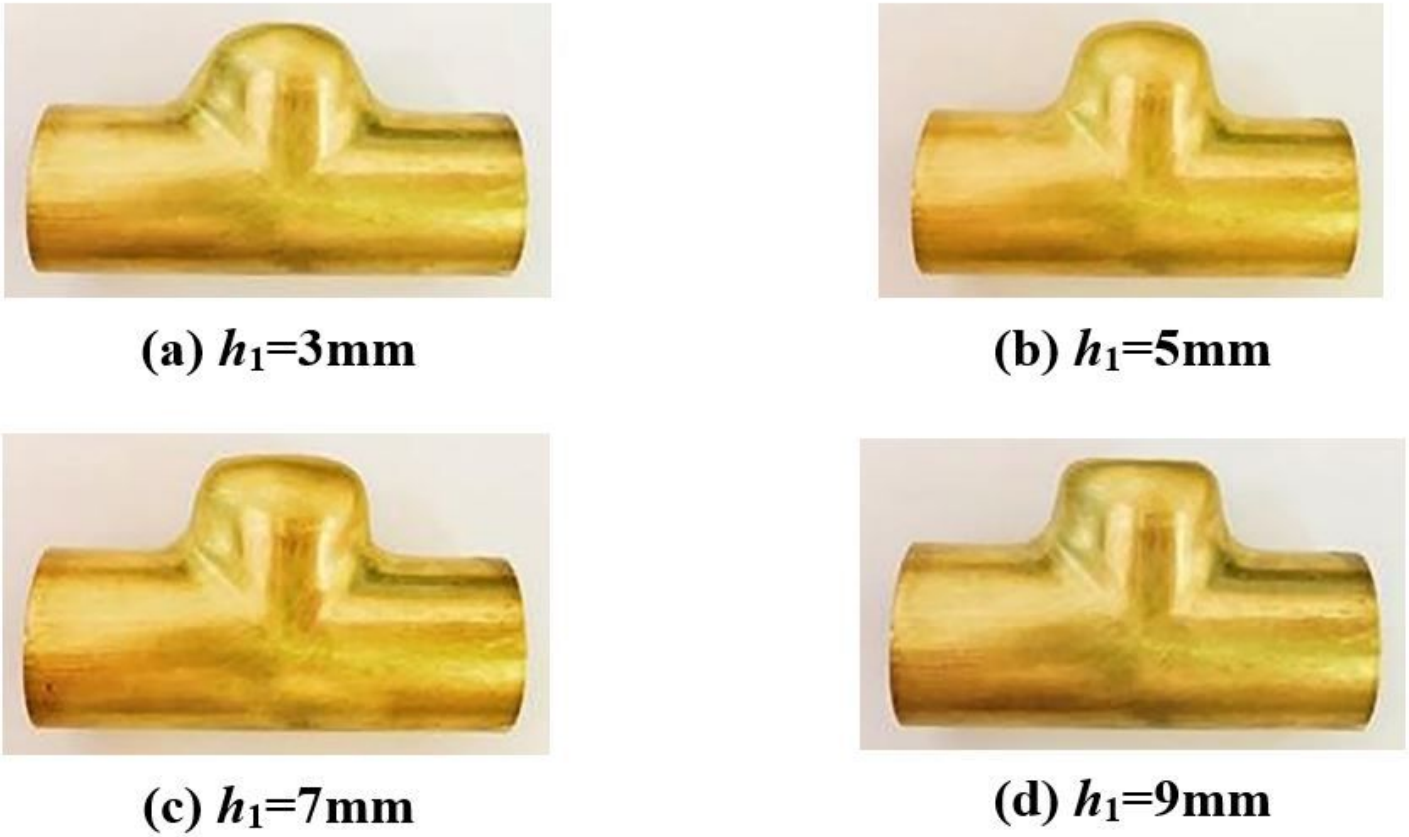

Figure 22

Photograph of T-shaped Tube Formed by Different Reverse Heights h1 in Experiments

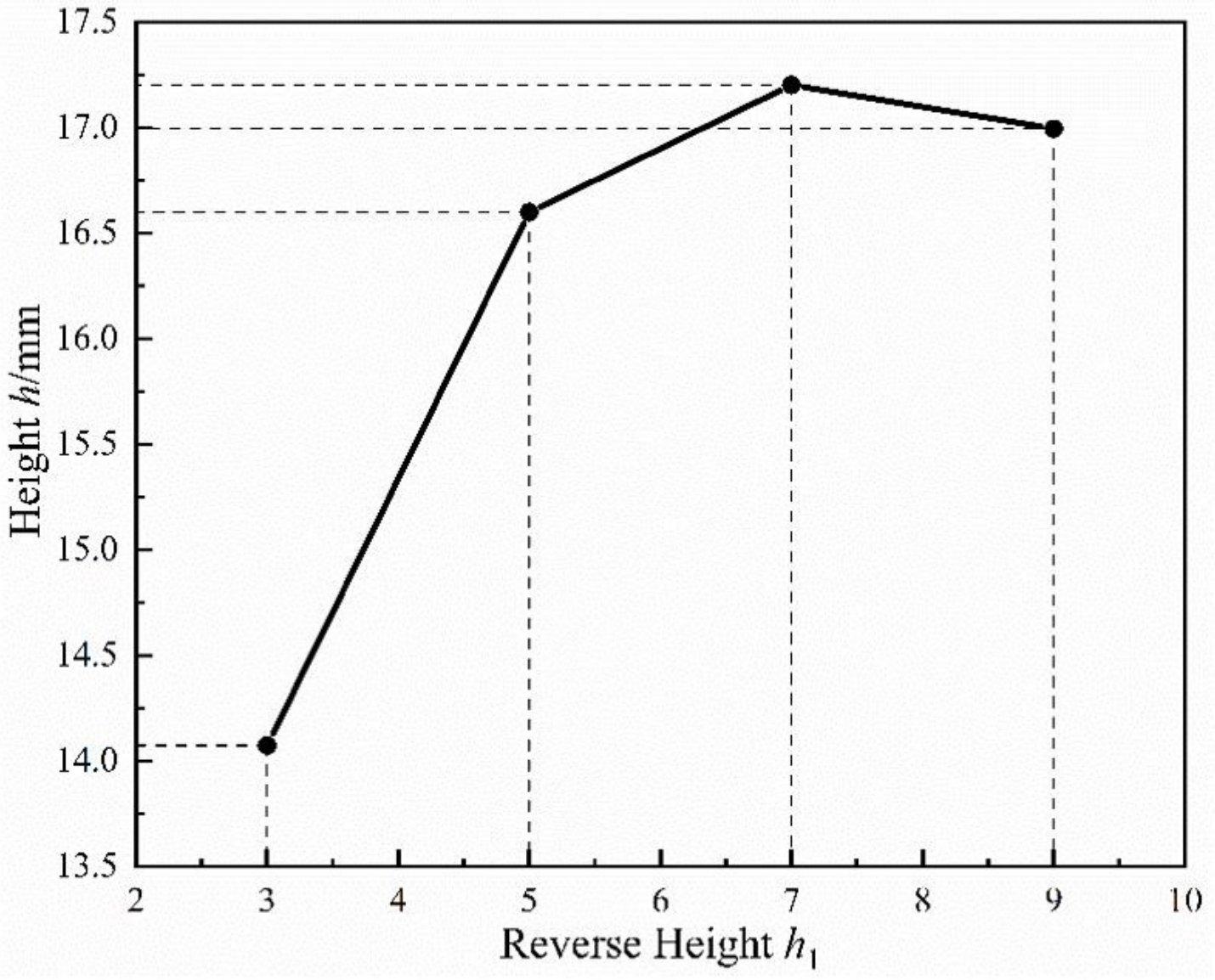

Figure 23

Height of T-shaped Tube Branch Formed by Different Reverse Height h1 in Experiments

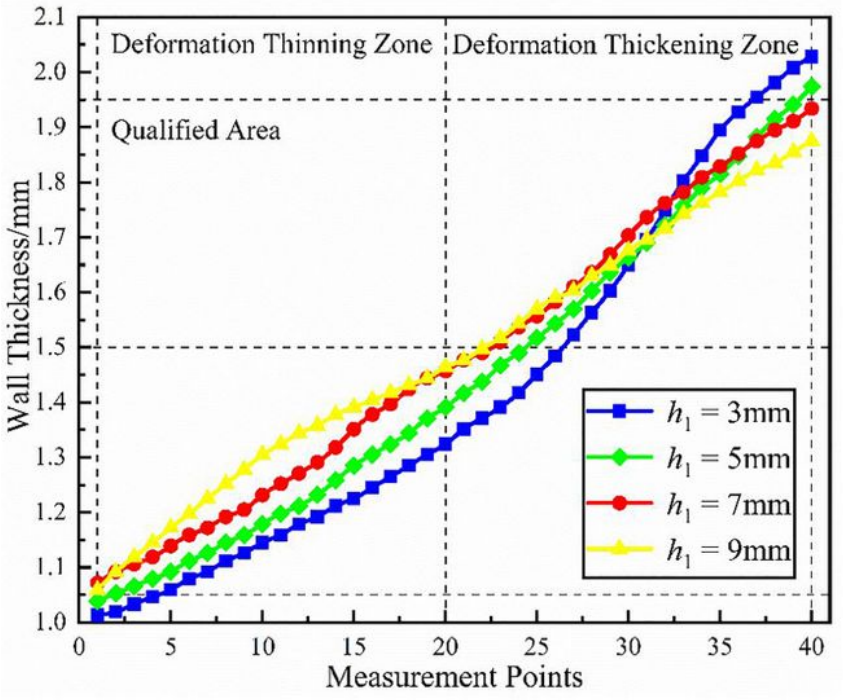

(a) Longitudinal Cross Section

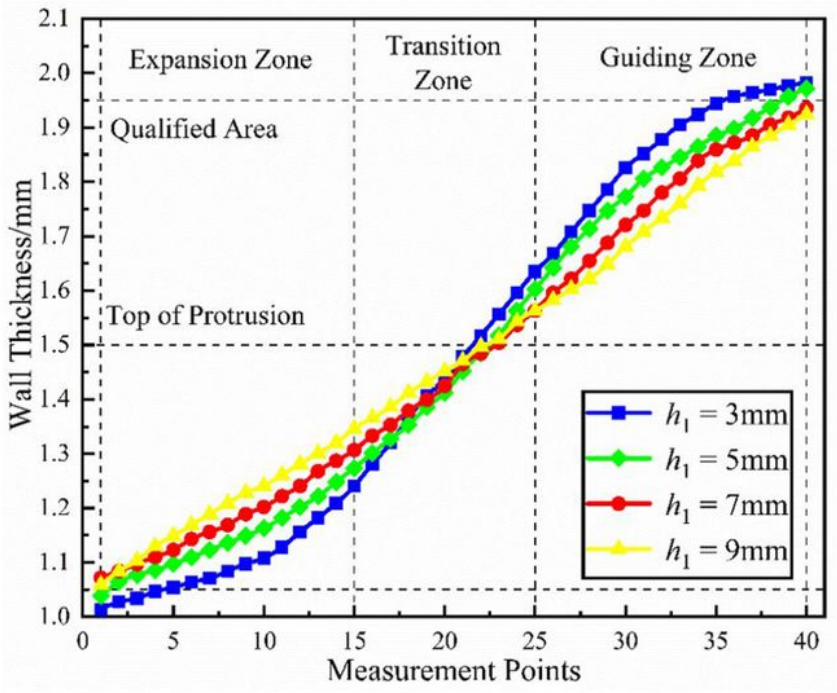

(b) Horizontal Cross Section

Figure 24

Wall Thickness Distribution of Cross Section of T-shaped Tube Formed by Different Reverse Height h1 in Experiments

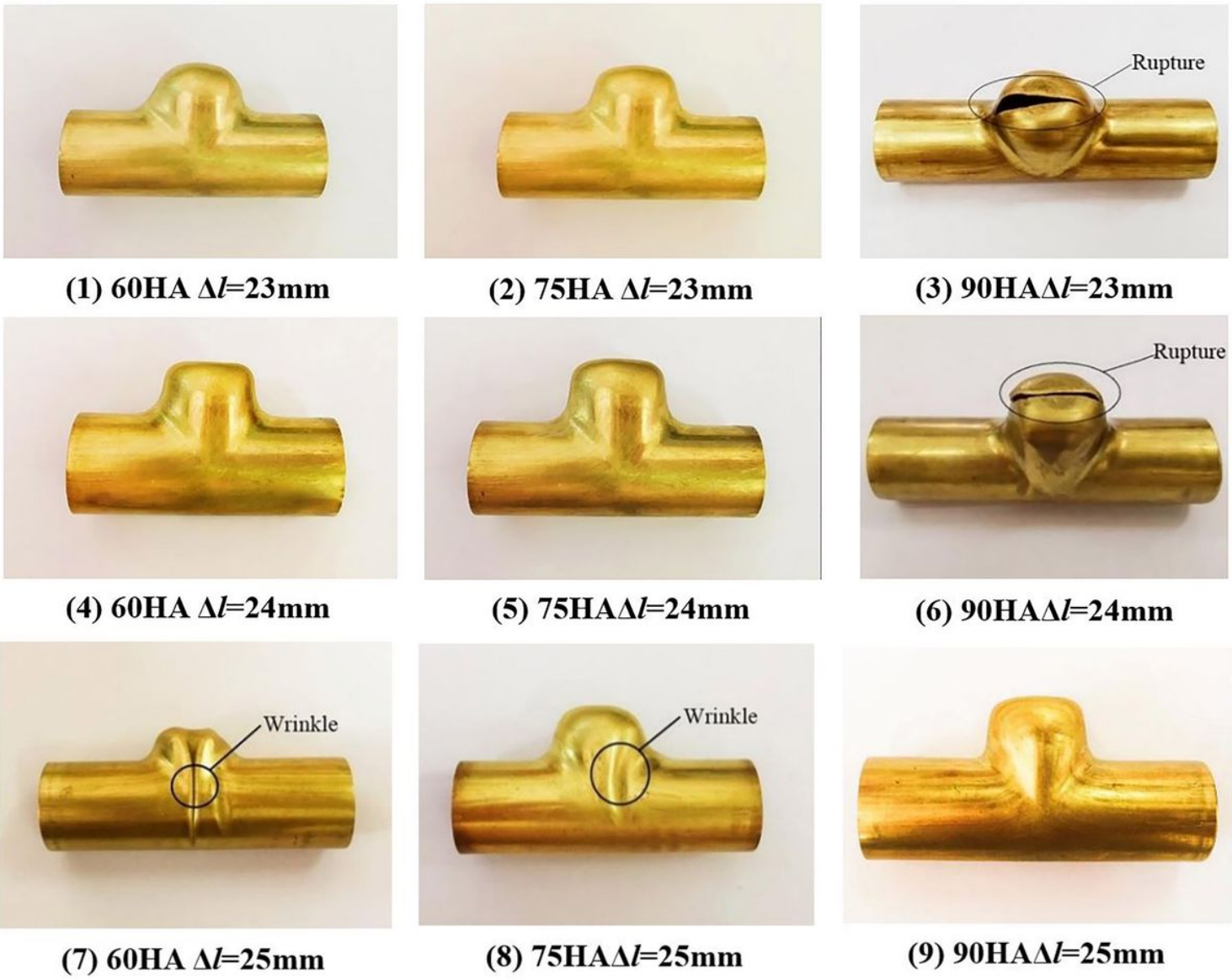

Figure 25

Photograph of T-shaped Tube Formed by Different Load Paths (MRRHAF) in Experiments

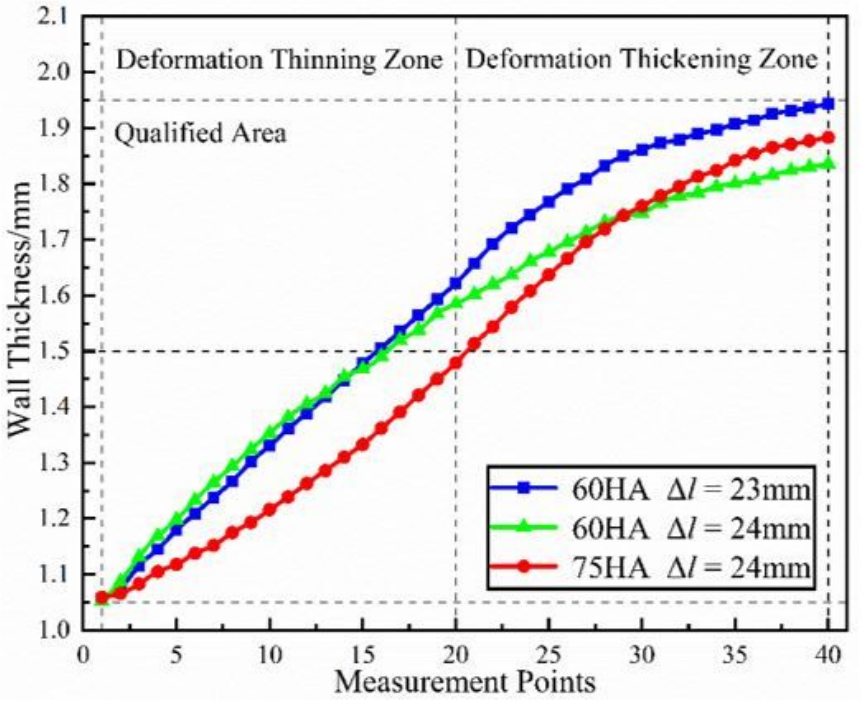

(a) Longitudinal Cross Section

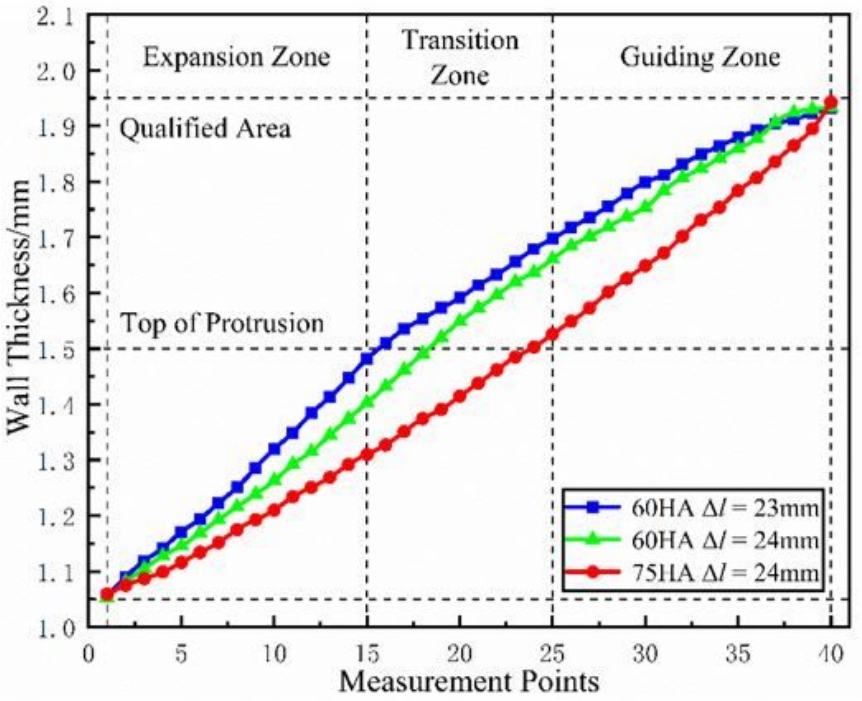

(b) Horizontal Cross Section

Figure 26

Wall Thickness Distribution of Cross Section of T-shaped Tube Formed by Different Load Paths (MRRHAF) in Experiments

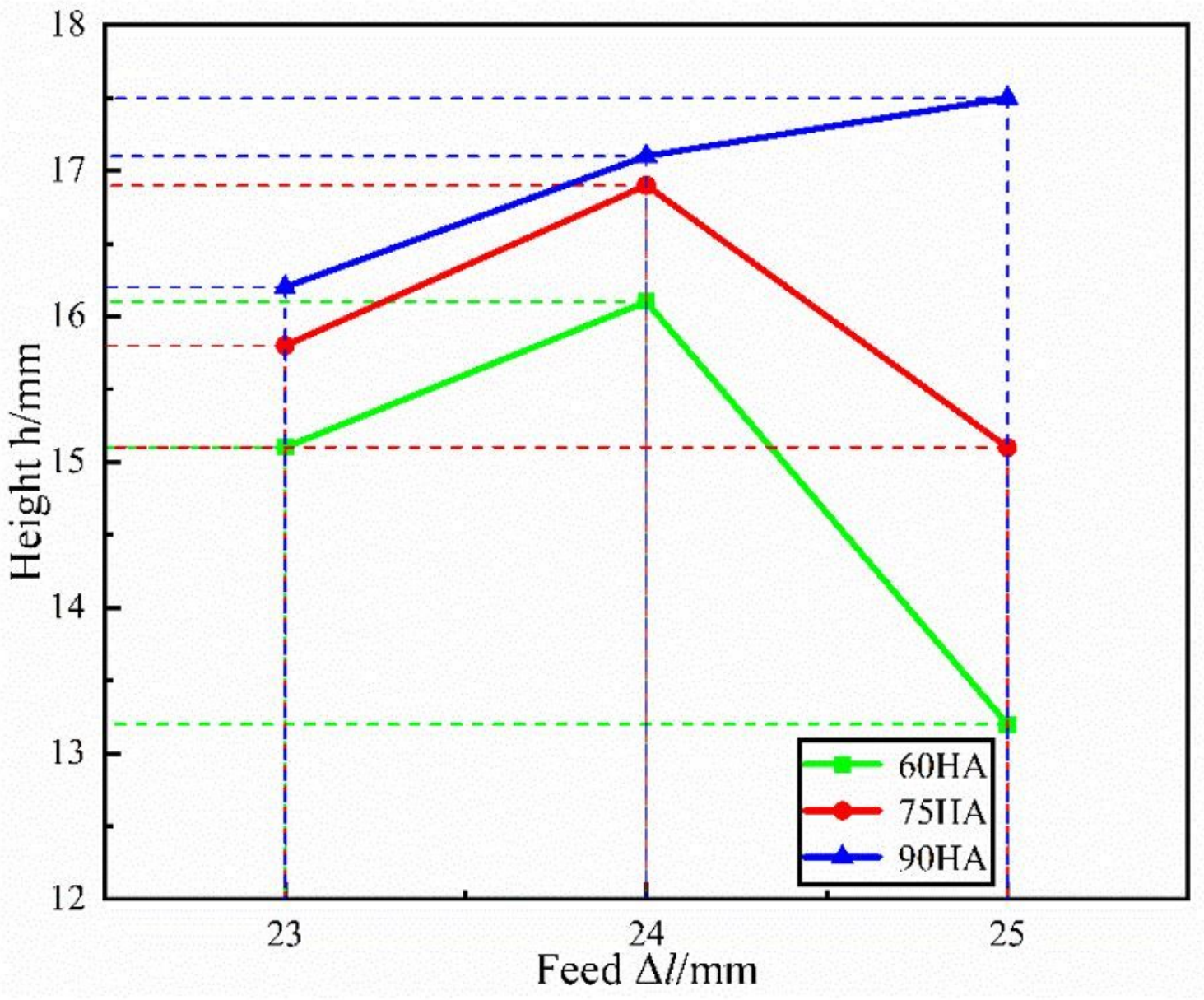

Figure 27

Relationship Between Rubber Hardness, Feed and Forming Height